VOT 75153

High Performance Computing Of Explicit Schemes For Electrofusion Joining Process Based On Message-Passing Paradigm

Halijah Binti Osman Norma Binti Alias Bahrom Bin Sanugi

Jabatan Matematik Fakulti Sains Universiti Teknologi Malaysia

2007

HIGH PERFORMANCE COMPUTING OF EXPLICIT SCHEMES FOR ELECTROFUSION JOINTING PROCESS BASED ON MESSAGE-PASSING PARADIGM

(PENGKOMPUTERAN BERKEMAMPUAN TINGGI BAGI SKEMA-SKEMA TAK TERSIRAT UNTUK PROSES PEMATRIAN ELEKTROFUSION BERDASARKAN PARADIGMA PERPINDAHAN DATA)

HALIJAH BINTI OSMAN
NORMA BINTI ALIAS
BAHROM BIN SANUGI

RESEARCH VOTE NO:
75153

Jabatan Matematik

Fakulti Sains

Universiti Teknologi Malaysia

2007

Lampiran 20

UTM/RMC/F/0024 (1998)

UNIVERSITI TEKNOLOGI MALAYSIA

BORANG PENGESAHAN
LAPORAN AKHIR PENYELIDIKAN

TAJUK PROJEK : **High performance computing of explicit schemes for electrofusion joining process based on message-passing paradigm**
vot: 75153, Ketua projek: Halijah Osman

Saya **HALIJAH OSMAN**
(HURUF BESAR)

Mengaku membenarkan **Laporan Akhir Penyelidikan** ini disimpan di Perpustakaan Universiti Teknologi Malaysia dengan syarat-syarat kegunaan seperti berikut :

1. Laporan Akhir Penyelidikan ini adalah hakmilik Universiti Teknologi Malaysia.
2. Perpustakaan Universiti Teknologi Malaysia dibenarkan membuat salinan untuk tujuan rujukan sahaja.
3. Perpustakaan dibenarkan membuat penjualan salinan Laporan Akhir Penyelidikan ini bagi kategori TIDAK TERHAD.
4. * Sila tandakan (/)

☐	SULIT	(Mengandungi maklumat yang berdarjah keselamatan atau Kepentingan Malaysia seperti yang termaktub di dalam AKTA RAHSIA RASMI 1972).
☐	TERHAD	(Mengandungi maklumat TERHAD yang telah ditentukan oleh Organisasi/badan di mana penyelidikan dijalankan).
✓	TIDAK TERHAD	

TANDATANGAN KETUA PENYELIDIK

Nama & Cop Ketua Penyelidik

CATATAN : ***** *Jika Laporan Akhir Penyelidikan ini SULIT atau TERHAD, sila lampirkan surat daripada pihak berkuasa/organisasi berkenaan dengan menyatakan sekali sebab dan tempoh laporan ini perlu dikelaskan sebagai SULIT dan TERHAD.*

PENGHARGAAN

Kami ingin mengucapkan terima kasih yang tak terhingga kepada pihak RMC UTM kerana memberikan geran penyelidikan jangka pendek kepada kami. Terima kasih juga kepada pihak Jabatan Matematik dan Fakulti Sains diatas sokongan yang diberikan.

ABSTRACT

The research focused on heterogeneous cluster workstations comprising of a number of CPUs in single and shared architecture platform. The problem statements under consideration involved one dimensional parabolic equations. The thermal process of electrofusion jointing was also discussed. Numerical schemes of explicit type such as AGE, Brian, and Charlie's Methods were employed. The parallelization of these methods were based on the domain decomposition technique. Some parallel performance measurement for these methods were also addressed. Temperature profile of the one dimensional radial model of the electrofusion process were also given.

ABSTRAK

Penyelidikan ini memberi focus kepada sistem gugusan stesen-kerja heterogenus yang mengandungi sebilangan CPU dalam platfom ingatan teragih dan berkongsi. Penyataan masalah yang dipertimbangkan melibatkan persamaan parabolik satu dimensi. Proses therma bagi pematrian elektrofusion juga dibincangkan. Kaedah berangka jenis tak tersirat seperti AGE, Brian, dan Kaedah Charlie telah diaplikasikan. Penselarian algoritma untuk kaedah-kaedah tersebut dibuat berasaskan kaedah teknik penghuraian domain. Ukuran pencapaian selari dijalankan terhadap kaedah-kaedah ini. Taburan suhu model satu dimensi bagi proses elektrofusion juga diberikan.

CONTENTS

LIST OF TABLES

LIST OF FIGURES

LIST OF ACRONYMS

Acronym	
EFW	Electrofusion Welding
SIMD	Single Instruction and Multiple Data
LAN	Local Area Network
POV-Ray	Persistence of Vision Raytracer
PE	Polyethylene
MRS	Minimum Required Strength
MDPE	Medium Density Polyethylene
ADI	Alternating Direction Implicit
AGE	Alternating Group Explicit
GSRB	Gauss Seidel Red Black
PVM	Parallel Virtual Machine

Chapter 1

Introduction

This chapter describes first the development of the parallel architecture followed by description on Electrofusion Welding (EFW)/Jointing.

1.1 Development of Parallel Architecture

The tool to run the prototype is based on heterogeneous distributed parallel computer systems. The research focuses on the Parallel Virtual Machine as the message-passing paradigm for the internal communication among processors. The definition of distributed memory is referred to the multiple processors operate independently but each has own private memory, data is shared across a communications networked using message passing paradigm. Memory is scalable to number of processors by increasing the number of processors, size of memory and bandwidth. Under the Flynn's taxonomy the distributed is classified as Single Instruction and Multiple Data Stream (SIMD) architecture. Where each instruction may operate on more than one data element, the intermediate host executed program logic and broadcasts the instruction to other processors.

1.1.1 High Performance Computing

High performance computing involves the use of distributed parallel computer systems based on a cluster of workstations. There are several advantages as given below.

1. Cheaper construction cost compared to shared memory multiprocessor architecture.
2. Large memory sizes are available to be used due to the combination of all physical memory from the processors.
3. Unlimited number of processors can be used.

4. The large computational problems can be solved more cost effectively by using the aggregate power and memory of many computers.

   The distributed parallel computer systems are available to solve any large-scale problems for graphic, sorting, visualization and scientific computing for education and researcher in science and engineering fields

1.1.2 Details on Development

The development and performance of a high performance computing are based on 38 PCs Intel Pentium IV and Intel Pentium III with 20GB hard drive. The development involves in the configuration of a cluster of workstations, developing Local Area Network (LAN) and installing the message-passing architectures using Parallel Virtual Machine environment (PVM) (Geist, et. al, 1994). A high performance computing is developed by using the heterogeneous 36 PCs. The structure of the parallel computer systems is shown in Figure 1 and the specifications are as follows:

1. 4 Processors Intel Pentium IV with 1.66 GHz speed.
   i. Two partitions hardisk Maxtor Diamond Max Plus 20GB
   ii. Two memory SDRAM 256 RAM
2. 32 Processors Intel Pentium III with 1 Ghz speed.
   i. One partitions hardisk Maxtor Diamond Max Plus 20GB
   ii. One memory SDRAM 128 RAM
3. Four Fujitsu monitors 15" (CRT Color Monitor)
4. 3Com Etherlink 10/100 PCI
5. Compaq Deskpro SBC.
6. Power supply SVX Pro 16

The network of the parallel computer systems is based on LAN. Our work has been carried out by workstations interconnected via Ethernet running TCP/IP with Internal network Intel 10/100 NIC. Table 1 show the IP address and host name of the workstation. LAN consists of the following:

1. Cable TRICOAX Combo KVM.

2. Cable UTP (unshielded Twisted Pair) Cat 5e.
3. D-Link DES-1024D 24-Port 10/100Mbps Switch
4. D-Link DI-804HV 4-Port Broadband VPN Router
5. 47Ux600mmx800mm E.Pack C/N

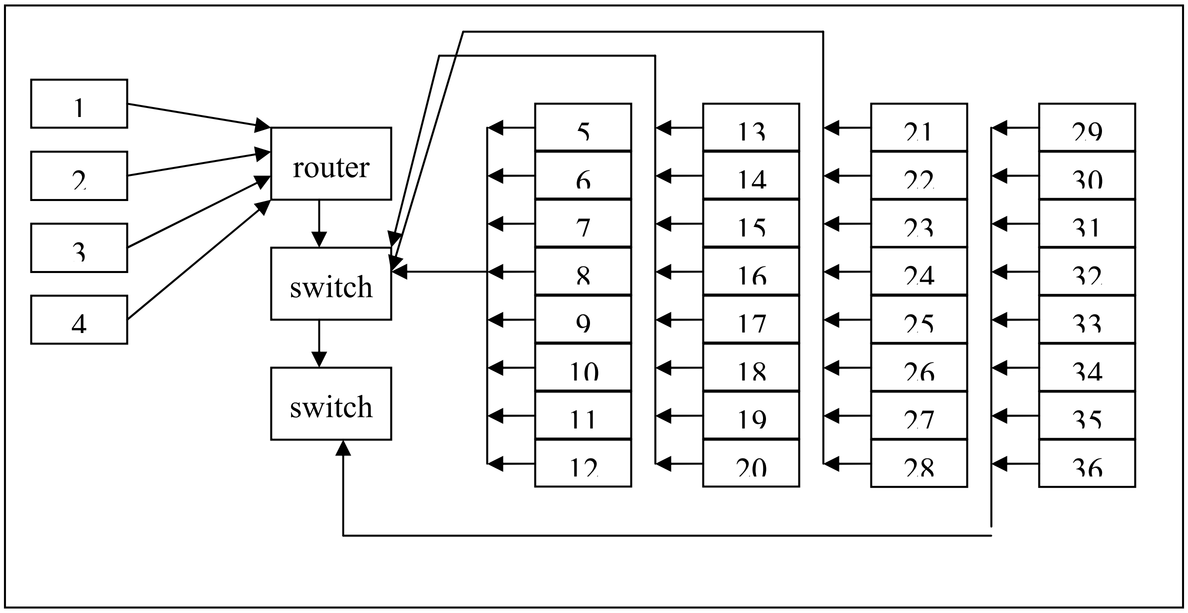

Figure 1: Local area Network of a high performance computing based on heterogeneous cluster workstation

Table 1: List of host name, domain name, and IP address of the workstation.

Host name	**Domain name**	**IP address**
norma1	norma1.cc.utm.my	10.1.1.1
norma2	norma2.cc.utm.my	10.1.1.2
norma3	norma3.cc.utm.my	10.1.1.3
norma4	norma4.cc.utm.my	10.1.1.4
norma5	norma5.cc.utm.my	10.1.1.5
.	.	.
.	.	.
.	.	.
norma36	norma36.cc.utm.my	10.1.1.36

The parallel computer systems are installed with PVM 3.4 version, MPI (MPICH version) and RedHat Linux 9. PVM is a library of functions addressable either from FORTRAN or from C, providing the means to communicate data among workstations as a whole. PVM can be implemented on different computer architecture, thus making it possible the integration of a heterogeneous cluster on workstations in a single virtual parallel computer. PVM has not been developed just for bringing together the workstations, but as a general programming tool on different message-passing architectures. Figure 3 shows the picture of a cluster on workstations in UTM.

1.1.3 Heterogeneous Cluster Workstation

A heterogeneous network (HN) can be abstracted as a connected graph HN (M, C), where M= $\{M1, M2,...,Mp\}$ is set of heterogeneous workstations (p is the number of workstations). The computation capacity of each workstation is determined by the power of its CPU, I/O and memory access speed. C is standard interconnection network for workstations, such as Fast Ethernet or an ATM network, where the communication links between any pair of the workstations have the same bandwidth.

Based on the above definition, if a network consists of a set of identical workstations, the system is homogeneous. Further, a heterogeneous network can be divided into two classes: a dedicated system where each workstation is dedicated to execute tasks of a parallel computation, and a non-dedicated system where each workstation executes its normal routines (also called owner workload), and only the idle CPU cycles are used to execute parallel tasks. In this paper we use a dedicated heterogeneous network of workstations.

1.1.4 Benchmarks

The distributed memory machine is tested on the POVBench Parallel Processor Benchmark. The standard programming is called PVMPOV (Jakob, 1994). The results are stated in Table 2, i.e the time execution versus number of processors in running the standard programming PVMPOV. Based on Table 1, the POVBench Parallel Processor benchmark shows that this machine is at position 59th of 2190 machines which is allocated 2.3% the best time in POVBench Parallel Processor Benchmark. The results can be searched on the Web page: http:www.haveland.com/index.htm?povbench/index.htm

1.1.4.1 PVMPOV

PVMPOV is short for the PVM and POV-Ray. *PVM* is a message passing system that enables a network of computers to be used as a single distributed memory parallel computer. This network is referred to as the *Parallel Virtual Machine*. *POV-Ray* is a 3-dimensional ray tracing engine. It takes information we supply and simulates the way light interacts with the objects we have defined to create stunning 3d pictures and animation which is called *rendering* process.

PVMPOV has the ability to distribute a rendering across multiple heterogeneous systems. Parallel execution is only active if the user gives the "+N" option to PVMPOV. Otherwise, PVMPOV behaves the same as regular POV-Ray and runs a single task only on the local machine. Using the PVM model, there is one master and many slave tasks. The master has the responsibility of dividing the image up into small blocks, which are assigned to the slaves. When the slaves have finished rendering the blocks, they are sent back to the master, which combines them to form the final image. The master does not render anything by itself, although there is usually a slave running on the same machine as the master, since the master doesn't use very much CPU power. If one or more slaves fail, it is usually possible for PVMPOV to complete the rendering. PVMPOV starts the slaves at a reduced priority by default, to avoid annoying the users on the other machines. The slave tasks will also automatically time out if the master fails, to avoid having lots of lingering slave tasks if we kill the master.

1.1.4.2 Installing PVMPOV

The instructions for the 3.1x version of POVray follow:

1. Download the UNIX sources for Povray from http://www.povray.org . For this paper, we used version 3.1g of POV-ray. These consist of two files povuni_s.tgz and povuni_d.tgz.
2. Download the PVMPOV patch file and store in home directory.
3. Create new directory for povray in *home* directory using the *mkdir* command. In our case, we create directory named *pvmpov3_1g_2*.

4. Copy the povray files into the *pvmpo3_1g_2* directory and *untar* them. This will create a directory called */povray31*.
5. From *home* directory *untar* the PVMPOV patch file. Change into the */pvmpov3_1g_2* directory.
6. Apply the patch by executing the *./inst-pvm* script.
7. Change into the */pvmpov3_1g_2/povray31/source/zlib* directory to compile the compression library. First run *./configure* script followed by command *make test*. Now *su* to become the root user temporarily and type *make install* to install the library. Type exit to become the normal user again.
8. Change into the */pvmpov3_1g_2/povray31/source/libpng* directory to compile the png library. Create the makefile by issuing the command: *cp scripts/makefile.std makefile*. Then type *make test*. When complete, issue the *su* command again and type *make install*. Type *exit* to become the normal user again.
9. Change into the */pvmpov3_1g_2/povray31/source/pvm* directory and modify the pvm.h file by changing the line *"#if defined(SUN4SOL2) || defined(your_pvm_arch)"* with *"#if defined(SUN4SOL2) || defined(LINUX)"*. On our cluster, we have to comment out the "*extern int setpriority..*". and "*extern int getpriority..*". lines from ~/povray3/source/pvm/pvm.h file. We figured this out by after several failed compiles.
10. The PVM_ARCH variable must be defined by adding *"export PVM_ARCH=LINUX"* in *.bash_profile* file.
11. Temporarily add the pvm library directory to your search path by entering "*export PATH=$PATH:$PVM_ROOT/lib*" also in *.bash_profile* file.
12. Now start the compile by entering "*aimk newunix*" from the */pvmpov3_1g-2/povray31/source/pvm* directory. When complete the PVMPOV executable will be in the */povray31/sources/pvm/LINUX* directory. Copy this to main home directory. Run *"aimk newsvga"* and *"aimk newxwin"* to generate the SVGA and X-windows versions respectively. Now repeat this on the remaining machines.

1.1.4.3 Running PVMPOV and Benchmarking

Copy the *skyvase.pov* file into the home directory of each of the computers running pvm.

1. Start *pvm* from one of your machines.
2. Add each of the other machines as before when we tested pvm. Type *conf* to confirm that they are all running.
3. Now type *quit* at the *pvm* prompt to drop back to the command-line. Note that the pvm daemon is still running.
4. With the cluster configured type the following to begin the raytracing:

```
./pvmpov +iskyvase.pov +h480 +w640 +FT +v1 -x -d +a0.300 -q9 -mv2.0 -b1000 -nw32
-nh32 -nt4 -L/root/pvmpov3_1g_2/povray31/include
```

This is the benchmark option command-line with the exception of the -nw and -nh switches, which are specific to pvmpov and define the size of image each of the slaves will be working on. The -nt4 switch is specific to the machine configuration. It starts four tasks, one for each CPU.

The messages on the screen should show that slaves were successfully started. The cluster is now rendering the image. When complete, PVMPOV will display the slave statistics as well as the total render time.

1.1.5 PVM

PVM is communication or message passing software which allows a heterogeneous collection of workstations or supercomputer to function as a single high-performance parallel machine. PVM is come prepackaged with most LINUX or Win32 install package on web page. There are three ways to start PVM:
1. PVM console-start, PVM or just attaches to running PVM.
2. Xpvm-PVM Graphical Interface includes graphical console and monitor for PVM.
3. pvmd-direct startup, seldom used expected for debugging.

1.1.5.1.1 POV-Ray

POV-Ray is short for the Persistence of Vision Raytracer, a tool for producing high-quality computer graphics. POV-Ray is copyrighted freeware. POV-Ray for Unix is essentially a version of the POV-Ray rendering engine prepared for running on a Unix or Unix-like operating system such as GNU/Linux. Ray-tracing is a rendering technique that calculates an image of a scene by simulating the way rays of light travel in the real world. Ray-tracing programs like POV-Ray start with their simulated camera and trace rays backwards out into the scene. The user specifies the location of the camera, light sources, and objects as well as the surface texture properties of objects, their interiors if transparent and any atmospheric media such as fog, haze, or fire.

Table 2: The time execution versus number of processors in running the standard programming PVMPOV

p	*t* (s)	Cost (RM)
1	13	5500
5	8	13000
10	7	28000
15	6	40500
20	6	53000
25	6	65500
30	5	78000
36	5	93000

Figure 2: The output visualization of skyvase using PVMPOV

Figure 3: A high performance computing system

1.2. Fusion Jointing

There are two basic systems of jointing polyethylene (PE) pipe underground and they are fusion methods and mechanical jointing. PE in various forms has been utilized by the gas and water industries in Europe as a pipeline material since 1956, due primarily to its high ductility, durability and weldability. One of the major attractions of polyethylene as a piping material is that it can be fusion welded. Fusion welds are made by bringing two molten surfaces together so that as they cool and recrystallize a welded joint forms at their interface. There are four types of fusion methods: Butt fusion, Socket fusion, Saddle fusion, and Electrofusion. The one that we are interested in is the Electrofusion technique.

1.2.1 Electrofusion Technique

Electrofusion is a technique used for creating joints between pipes made of plastic material. The principle underlying electrofusion is simple. It is based on incorporating an electric coil into a fitting very close to the interface to be welded. An electric current is run through the coil in order to heat it, using the Joule effect. This causes the material to melt slowly. The joint is complete once the area has cooled.

The heating element, which may or may not be coated, is made from metallic material ranging from pure copper and brass to manganese-nickel alloy. Normally the coating is the same material as used to manufacture the fitting. Bowman (1997) noted that EF fittings operating at an alternating voltage below or equal to 80V are usually used for buried gas and water pipes system while those operating at 220V are used in above-ground applications. These ratings are for larger dimension fittings. For fittings up to 180 mm nominal diameter the alternating voltage is 40V rms.

1.2.2 Electrofusion Fittings

EF fittings are commonly manufactured from polymeric materials, usually PE80 and PE100 compounds based on polyethylenes with a density no less than 930 kg/m^3. The minimum required strength (MRS) that could sustain pipe hoop stresses are 8\, MPa and 10\, Mpa respectively. The MRS value is important in designing pipe systems as it ensures that a typical design life of 50 years is achieved (Bowman, 1997; Rosala, 1995). Rosala (1995) gives the relationship of MRS value and maximum allowable hoop stress as σ = MRS/C where C is the overall service coefficient.

There are two types of EFW fittings: the patch-form, or saddle fitting, and the barrel-form. Various examples of these fittings are shown in Figure 4.

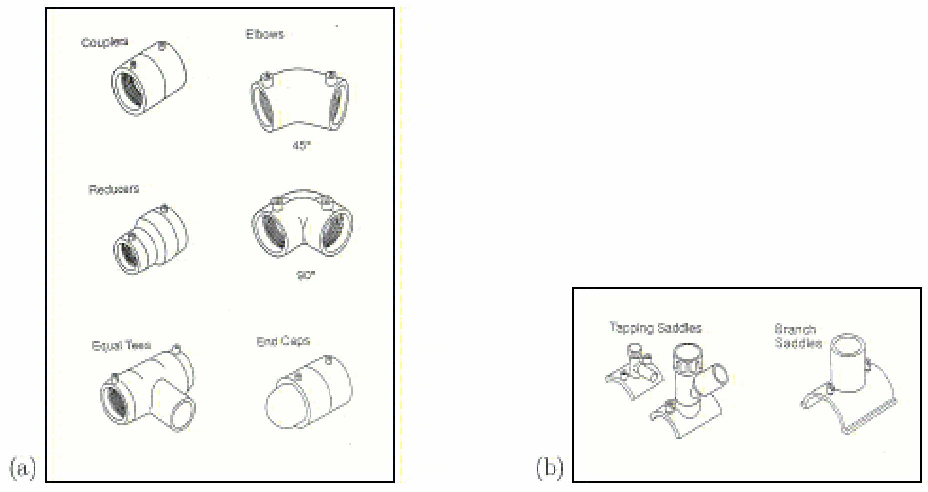

Figure 4: Electrofusion fittings (a) barel-form (b) patch-form (Rosala, 1995)

Although there are several different wire-embedding technologies, about 99.99% of EFW pipe fittings use an implanted or moulded-in resistance heating wire (Bowman, 1997). The subject of the present study is the barrel-form fitting in which the shape is axially symmetric and the heating coil is usually wound in a monofilar manner as shown in Figure 5. Specifically we are interested in a coupler that is thermoplastic and of polyethylene type. Usually the coupler has a constant bore along its length, larger than that of the pipe. This is referred to as a clearance design in Figure 6.

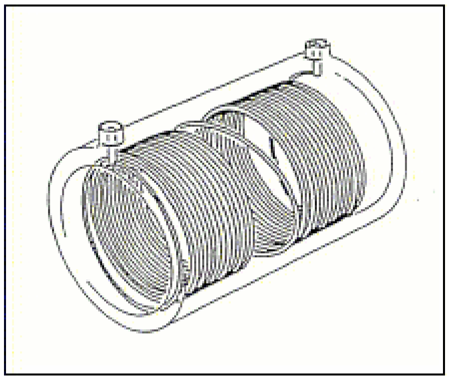

Figure 5: Monofilar winding in a barrel-form coupler (Rosala, 1995)

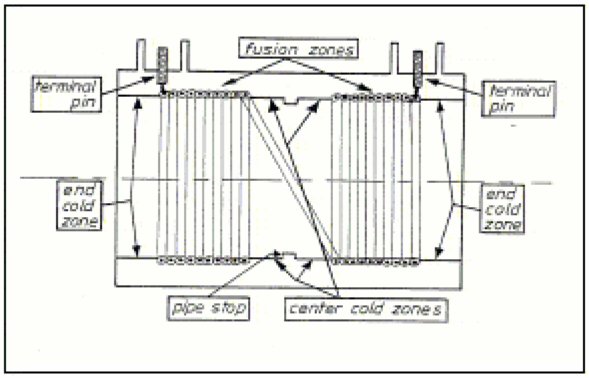

Figure 6: Schematic diagram of a coupler (Bowman, 1997)

1.2.3 Jointing Process

Fusion jointing of PE pipe systems using EF fittings is rapidly gaining preference over the older butt and socket fusion techniques. The reasons include

1. an ability to join the widest range of PE pipe grade resins,

2. narrow trench technology can be used,
3. joints are correctly positioned and assembled prior to fusion, and
4. reported joint failure are very low, at rate of 3 per 10000 joints (Bowman, et. al, 1992).

To significantly assist in the creation of a strong EF joint, various pipe preparation steps should be followed before the joining process starts (Bowman, 1991).

1. The outer wall of the pipe must be scraped (or cleaned) to obtain a good weld quality. This was confirmed from studies by Misaka et. al (1993) in which they suggested using acetone or an electric scraper to remove contaminants such as dirt and oxidised plastic. However Morris and Gill (1991) cautioned that brittle joint failures were more common for 180mm pipe in standard test pieces in which the clearance between the pipe and coupler exceeded 1.3mm. Furthermore, a large clearance affects the expansion during the heating phase leading to insufficient interface pressure needed for a good joint (Donoghue et.al, 1991).
2. The two pipe ends must be pushed against the pipe stops to ensure that molten plastic does not enter the pipe interiors.
3. The pipes and fitting should be securely clamped to eliminate relative material movements and to ensure that the melted polymer is contained at the fusion interface. This results in low stress factors in the welding plane, even with two resins of different origins (Usclat, 1985), hence facilitating a strong joint.

The EF jointing process can then be commenced and it is well described by Bowman (1991) in three main phases.

1. **Initial heating**: After completing the pipe preparation procedures an alternating current is passed through the wire surrounding the fusion zones. Typically an initial air gap (clearance) is present between the pipe and coupler (Figure 7a). Temperature increases due to Joule heating creates the heat to expand the polymer into the fitting bore. The total energy dissipated over the total fusion area is usually controlled by passing the current for a known fixed time even though other methods do exist (Usclat, 1985). Eventually the air gap closes due to thermal expansion (Figure 7b).

This phase consumes between 20% and 40% of the total fusion time (Bowman, 1991).

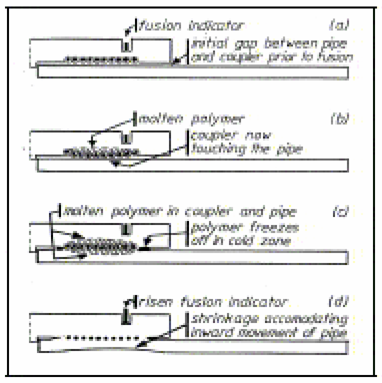
fusion indicator
(a)
initial gap between pipe and coupler prior to fusion
molten polymer
(b)
coupler now touching the pipe
molten polymer in coupler and pipe
(c)
polymer freezes off in cold zone
risen fusion indicator
(d)
shrinkage accomodating inward movement of pipe

Figure 7: Stages in the formation of an electrofusion joint (Bowman, 1991)

2. **Heat soak and fusion jointing**: Thermal contact causes the heat energy from the wire to be distributed to create a melt pool at the fusion interface. A carefully controlled and correctly identified energy input and the low thermal conductivity of PE help the coupler and pipe to contain the melt. On further heating, the contained melt pool increases to build up melt pressure. Cold zones located at either side of the fusion zones are crucial to the build up of molten polymer and melt pressure. They act as a barrier to block off any molten polymer that is trying to escape (Figure 7c). Eventually the fusion joint between the pipe and coupler is formed as a result of the combined action of the heat and pressure. The pressure developed at the fusion interface is recognized as a major contributing factor for generating a good bond along the EF joint (Fujikake et. al, 1997; Kanninen et.al, 1992; Donoghue et. al, 1991).
3. **Cooling**: This process begins when the current is turned off. The cold zones solidify any molten polymer that attempts to extrude out whilst the melt at the interface slowly cools and contracts. The contraction on cooling is accomplished by allowing motion of the pipe towards the fitting (Figure 7d).

1.2.4 **Simulation Model**

Fusion simulation is one of the key techniques used in designing and producing electrofusion joints. This is because performing comprehensive experimental studies in some instances can be an expensive exercise. An alternative is to use a computer simulation of the electrofusion process to suggest suitable designs that may then be tried experimentally. Such a computer simulation need not necessarily include all the complexities of the electrofusion process providing it can be used to point the designer in the correct direction. For that, mathematics is used to model the thermal fusion process which is then solved analytically or numerically. Normally, problems of this type are highly nonlinear and no analytical solution is found so far. As such numerical technique is unavoidable.

In this report we shall assume circular symmetry which will facilitate the development of a one-dimensional radial model for the electrofusion process. Consider a one-dimensional section through a hollow thick-walled cylindrical body exhibiting axial symmetry. Admitting temperature dependent thermal properties λ (thermal conductivity), ρ (density) and c (specific heat) leads to the nonlinear radial heat diffusion equation

$$\rho_i\, c_i\, \frac{\partial U_i}{\partial t} = \frac{1}{r}\frac{\partial}{\partial r}\left(\lambda_i(U_i)\, r\, \frac{\partial U_i}{\partial r}\right)$$

in which $U_i(r,t),\ i=f,p$ is the temperature at a fixed point *x* and time t for the fitting (*f*) and pipe (*p*) respectively. The nonlinearity of this equation is made explicit by expanding the derivatives on the right-hand side to obtain

$$\rho_i\, c_i\, \frac{\partial U_i}{\partial t} = \lambda_i\left(\frac{\partial^2 U_i}{\partial r^2} + \frac{1}{r}\frac{\partial U_i}{\partial r}\right) + \frac{d\lambda_i}{dU_i}\left(\frac{\partial U_i}{\partial r}\right)^2 .$$

To simplify matter, this report concerns with the linear case only. Thus the problem reduces to the following model equations

$$\rho_i\, c_i\, \frac{\partial U_i}{\partial t} = \lambda_i\left(\frac{\partial^2 U_i}{\partial r^2} + \frac{1}{r}\frac{\partial U_i}{\partial r}\right) .$$

Heat transfer at the outer surface of the fitting and the inner surface of the pipe is by convection. An explicit finite difference solution based on control volume method is used to solve the equations.

Besides the radial form of the parabolic PDE, we also employed linear heat equation in the Cartesian coordinates system, given in the dimensionless form by

$$\frac{\partial u}{\partial t} = \frac{\partial^2 u}{\partial x^2}$$

We use this to test-run our numerical methods.

Chapter 2

Literature Review

2.1 Parallel and Distributed Computing

The field of parallel and distributed computing, like many emerging disciplines, has both promoters and detractors. It seems nowadays accepted that parallel computing is the most promising venue for High Performance Computing. Many forms of parallelism exist today, from architectures designed around the idea of bringing together a relatively small number of very tightly-coupled processors, to where the coupling is relatively loose. However, the number of processors can scale up to thousands, getting us into massive parallelism. In general, the practical implementation of any of this parallel computer leads to relatively expensive machines that, presently, seldom exist at the Departmental level.

Recently, two technological breakthroughs have permitted the proposal of another approach to what a parallel computer could be. The availability of very fast processors in modern workstations, besides the widespread utilization of networks, has lead to the suggestion of designing a "virtual parallel computer" bringing together a number of these fast workstation by means of a Local Area Network (LAN), this is what we mean by Distributed Parallel Computer Systems. Heterogeneous in general means something consisting of dissimilar elements or parts.

2.2 Numerical Simulation of EFW

With the advance of computer technology, simulation has become a necessary tool in most research involving industrial application, such as EFW. Expensive testing and time consuming work for developmental purposes can be avoided by implementing combined mathematical modelling and simulation codes based upon the sound description of the process. A majority of researchers in EFW have employed FE simulation codes which are a popular tool for stress analysis. FD is more suitable for tackling fluid flow problems.

This section presents a review of published works on the numerical simulation of EFW process models.

Significant research work in EFW was only begun in the 1980s. Active participating countries include the United Kingdom, France, Japan and the United States. Attempts to numerically model the process probably started in the mid 1980s when Pitman (1985), from the BP Chemical Ltd., presented his work at the Plastics Pipes VI conference (University of York, UK). This appears to be the first published numerical simulation work concerning the EFW process model. Temperature constitutes an essential welding parameter and much of the published work simply dealt with this heat transfer process.

Pitman (1985) constructed a one-dimensional cartesian heat transfer model of a coupler by looking at the system from an axial point of view and simplifying geometrical domain to comprise a long rectangular layer of fitting, a heated layer, an interface and a pipe. The model took into account temperature dependent material properties and the EFW process was based on three assumptions:

1. a one-dimensional analysis is assumed since the area covered by the heater is very much greater than the thickness of the fitting and the pipe,
2. the temporary presence of the air gap between the fitting and the pipe does not significantly affect the heat transfer process, and
3. the energy supplied by the heater is distributed evenly through a layer of width equal to the diameter of the wire.

His transport equation accounting for heating is of the form

$$\frac{\partial}{\partial x}\left(k(T)\frac{\partial T}{\partial x}\right) + H(T,t) = \rho(T)c_p(T)\frac{\partial T}{\partial x}$$

for the heating layer and $H = 0$ within the polymer, with different thermal properties between them. He then applied convective cooling boundary conditions at the fitting's outer surface and at the pipe bore and solved the models using an implicit finite difference method. Pitman's model may have paved the way for tackling thermal problems in the EFW process, but he ignored one of the most important parameters that is typical of the EFW system - the presence of an air gap (clearance). Further he did not account for polymer deformation, and ignoring curvature he missed the term

$$\frac{1}{x}\frac{\partial T}{\partial x}$$

in the temperature calculation which might be significant for small couplers.

Using the same geometrical approach as Pitman, and neglecting air gap between the pipe and coupler, Dufour and Meister (1989) from Gaz de France proposed an improved model by considering latent heat effects in the heat transfer equations. They utilized both FE and FD. Their nonlinear enthalpy model accounting for phase change

$$\frac{\partial H(T)}{\partial t} - \mathrm{div}[k(T)\mathrm{grad}(T)] = 0$$

was solved by a special FE package Ali-baba, developed by Direction des Etudes et Recherches d'Electricit'e de France. Their linear 1D model

$$\frac{\partial T}{\partial t} = a_i \frac{\partial^2 T}{\partial x^2}; \quad i = s\ (\text{solid}), l\ (\text{liquid})$$
$$\frac{\partial T}{\partial t} = a_s \frac{\partial^2 T}{\partial x^2} + W; \quad \text{interface}$$
$$\frac{\partial T}{\partial t} = a \frac{\partial^2 T}{\partial x^2} + E; \quad \text{heating area}$$

was solved using explicit finite difference (FD) methods. The comparison of the two methods with experiment showed that the experimental results were an average of the two methods. Again, although the methodology of Dufour and Meister is much better, they also ignored deformation and did not fully implement the correct cylindrical geometry.

Other early numerical studies that contributed to the understanding of EFW processes were undertaken by Saint-Royre et al (1989), Nussbaum et al (1991) and Nakano et al (1989). Saint-Royre et al also from Gaz de France investigated the general fusion welding problem and their experiment suggested that the bonding at the fusion interface was probably governed by macromolecular interdiffusion. They developed a numerical model of a medium density polyethylene (MDPE) resin based upon the theory of macromolecular interdiffusion and computed the minimum temperature for an optimum weld (joint quality) as a function of heating time. The diffusion parameters were determined by a graphical method. Nussbaum et al (1991) continued the research to cater for the weldability of different pairs of resin types.

Nakano et al (1989) ran FE analyses based upon the Adina code and performed using a linear-elastic 3D theory. The analyses focused on evaluating stress concentrations at the heating wire zone and edges of an EF saddle and socket subjected to internal pressure and bending. Their work indicated that the difference in stress concentrations of the two types of fittings is not substantial and that the heating element has little influence on estimating the maximum stress in EF Fittings. To verify the adequacy of the FE results they performed fatigue tests and concluded that EF fittings posseses long-term resistance against internal pressure and external loads, guaranteeing the long-term reliability of EF fitting systems.

Returning to procees modelling, O'Donoghue et al (1991) and Kanninen et al (1992) produced simulation analyses using a commercial general purpose FE package, Abaqus. The work formed part of an ongoing research project sponsored by the Gas Research Institute (USA) to enhance the EF joining technique for the U.S. gas industry. They claimed that their 1D axisymmetric model is valid based upon the assumption that the temperature distribution in the centre of the wire region is relatively independent of axial effects. Thus they worked on a 1D thermo-mechanical analysis including temperature dependent material properties, latent heat effects, and initial clearance. Nevertheless, by ignoring axial effects, they have not fully described the heat transfer process.

Nakashiba et al (1993) and Nishimura et al (1992, 1994) went closer to reality by establishing a two-dimensional nonlinear heat transfer model with phase change based upon the Castem FE code. They used a cylindrical coordinate system and studied the effects of applied voltage, heating time, wire pitch, and ambient temperature for large 150mm sockets based on a 50mm EF socket. However, they ignored the presence of the air gap in their analysis.

Realizing that the implementation of sophisticated FE codes such as Abaqus are computationally expensive, some reseachers have resorted to other methods, particularly FD. Among them Wood et. al (1994) conducted a preliminary study of thermoelastic deformation using FD techniques for a one-dimensional radial model undergoing a change of phase. The presence of the air gap was also included. Their nonlinear model accounting for phase change had the form

$$\frac{\partial Q}{\partial t} = \rho\, c\, \frac{\partial U}{\partial r}\frac{dr}{dt} + K\left(\frac{\partial^2 U}{\partial r^2} + \frac{1}{r}\frac{\partial U}{\partial r}\right) + \frac{dK}{dU}\left(\frac{\partial U}{\partial r}\right)^2$$

and was solved using an explicit FD method. Polymer deformation was computed based on linear thermal expansion. They demonstrated that a fast, adequate, and efficient thermo-mechanical code can be generated. Their approach of using a variable space grid is, however, not necessary.

From the literature survey, numerical studies of EFW process based on FE codes are far ahead of FD-based studies. To some extent the thermo-mechanical analysis of elastic models is almost complete. On the other hand, FD-based computation of elastic models has so far centred around thermal models indicating that further research is required.

Chapter 3

Methodology

3.1 Parallel Algorithms

In Alias,Sahimi and Abdullah (2002), the six strategies of parallel algorithms in solving heat equation are implemented. These strategies were found to be more effective using the cluster of workstations. In this paper, the research focuses on the Conjugate Gradient (CG) for Alternating Group Explicit Method (AGE) in solving one dimensional heat conductor equation.

Topics will include Alternating Group Explicit-Conjugate Gradient Method (AGE_CG) and its parallel strategies. AGE_CG has been created using the acceleration technique and the parallelization of AGE_CG is achieved by domain decomposition technique on non-overlapping subdomain. The computational analysis of the proposed strategies are presented by using explicit *(2x2)* block systems.

3.1.1 AGE Method

By the Alternating Direction Implicit (ADI), AGE methods with Peaceman-Rachford variation is created to be more extremely powerful, flexible and affords its users many advantages. The accuracy of this method is comparable if not better than that of the GE class of problems as well as other existing schemes (Evans and Abdullah, 1983). The

$$\begin{aligned} u^{(k+\frac{1}{2})} &= (\mathbf{G}_1 + rI)^{-1}[(rI - \mathbf{G}_2)u^{(k)} + \mathbf{f}] \\ u^{(k+1)} &= (\mathbf{G}_2 + rI)^{-1}[(rI - \mathbf{G}_1)u^{(k+\frac{1}{2})} + \mathbf{f}] \end{aligned}$$

development of AGE with (2,2) accuracies is based on time level splitting strategy and the implicit form are as follows, and to implement the AGE method, we split the coefficient matrix A given as,

$$\mathbf{A} = \mathbf{G}_1 + \mathbf{G}_2$$

$$\mathbf{G}_1 = \left[\begin{array}{c|cc|cc|cc|cc}
a/2 & & & & & & & & \\
\hline
 & a/2 & b & & & & & & \\
 & c & a/2 & & & & & & \\
\hline
 & & & a/2 & b & & & & \\
 & & & c & a/2 & & & & \\
\hline
 & & & & & \ddots & & & \\
 & & & & & & \ddots & & \\
\hline
 & & & & & & & a/2 & b
\end{array}\right.$$

$$\mathbf{G}_2 = \left[\begin{array}{cc|cc|cc|cc|c}
a/2 & b & & & & & & & \\
c & a/2 & & & & & & & \\
\hline
 & & a/2 & b & & & & & \\
 & & c & a/2 & & & & & \\
\hline
 & & & & \ddots & & & & \\
 & & & & & \ddots & & & \\
\hline
 & & & & & & a/2 & b & \\
 & & & & & & c & a/2 & \\
\hline
 & & & & & & & & a/2
\end{array}\right]_{m\times m}$$

since $\mathbf{G}_1$ dan $\mathbf{G}_2$ are simply composed of (2×2). The alternating implicit nature of the (2×2) groups where the implicit and explicit values are given on the forward and backward levels for sweeps on the $(k+\frac{1}{2})^{th}$ and $(k+1)^{th}$ levels, with $r_1 = r - \frac{a}{2}$, $r_2 = r + \frac{a}{2}$ end $\Delta = r_2^2 - bc$. The experimental values of r were obtained within $0 \leq r \leq 1$ by running the programming for different value of r and choosing the one(s) that gave the minimum number of iterations. Each iteration is split into 2 intermediate level in parallel separated by a synchronizing call. This to ensure the updates in $(k+\frac{1}{2})^{th}$ sweep are completed before the updates in the $(k+1)^{th}$ sweep begin. Thus the parallel algorithm of AGE is stated as follows,

i. at the $(k+\frac{1}{2})^{th}$ iterate

$$
\begin{aligned}
u_1^{(k+\frac{1}{2})} &= \frac{r_1 u_1^{(k)} - b u_2^{(k)} + f_1}{r_2} \\
u_i^{(k+\frac{1}{2})} &= \frac{A u_{i-1}^{(k)} + B u_i^{(k)} + C u_{i+1}^{(k)} + D u_{i+2}^{(k)} + E_i}{\Delta} \\
u_{i+1}^{(k+\frac{1}{2})} &= \frac{\widetilde{A} u_{i-1}^{(k)} + \widetilde{B} u_i^{(k)} + \widetilde{C} u_{i+1}^{(k)} + \widetilde{D} u_{i+2}^{(k)} + \widetilde{E}_i}{\Delta}
\end{aligned}
$$

with $i = 2, 4, 6, ..., m-1$, $A = -cr_2$, $B = r_1 r_2$, $C = -br_1$, $E_i = r_2 f_i - b f_{i+1}$,
$D = \{^{o,i=m-1}_{b^2,i\neq m-1}$
and $\widetilde{A} = -cr_2$, $\widetilde{B} = r_1 r_2$, $\widetilde{C} = -br_1$, $\widetilde{E}_i = r_2 f_i - b f_{i+1}$,

$\widetilde{D} = \{^{o,i=m-1}_{-br_2,i\neq m-1}$

ii. at
$$
\begin{aligned}
u_i^{(k+1)} &= \frac{P u_{i-1}^{(k+\frac{1}{2})} + Q u_i^{(k+\frac{1}{2})} + R u_{i+1}^{(k+\frac{1}{2})}}{\Delta} \\
&+ \frac{S u_{i+2}^{(k+\frac{1}{2})} + T_i}{\Delta} \\
u_{i+1}^{(k+1)} &= \frac{\widetilde{P} u_{i-1}^{(k)} + \widetilde{Q} u_i^{(k)} + \widetilde{R} u_{i+1}^{(k)} + \widetilde{S} u_{i+2}^{(k)} + \widetilde{T}_i}{\Delta} \\
u_m^{(k+1)} &= \frac{-c u_{m-1}^{(k+\frac{1}{2})} + r_1 u_m^{(k+\frac{1}{2})} + f_m}{r_2}
\end{aligned}
$$

with $Q = r_1 r_2$, $R = -br_1$, $S = b^2$, $T_i = r_2 f_i - b f_{i+1}$,
$\widetilde{P} = \{^{o,i=1}_{c^2,i\neq 1}$
and $\widetilde{Q} = -cr_1$, $\widetilde{R} = \widetilde{Q} = r_1 r_2$, $S = -br_2$, $\widetilde{T}_i = -c f_i + r_2 f_{i+1}$.

3.1.2 Brian Methods

Linear Interpolation is exploited to accelerate the convergence and efficiency of BRIAN method. Through the Alternating Direction Implicit (ADI), BRIAN method is created to be more powerful, flexible and it offers users many advantages. The set of equations for the computation of the BRIAN method takes the form,

$$
\begin{aligned}
(rI + \mathbf{G}_1) u^{(k+\frac{1}{4})} &= (rI - \mathbf{G}_2) u^{(k)} + \mathbf{f} && (6) \\
(rI + \mathbf{G}_2) u^{(k+\frac{1}{2})} &= r u^{(k+\frac{1}{4})} + \mathbf{G}_2 u^{(k)} \\
u^{(k+1)} &= 2u^{(k+\frac{1}{2})} - u^{(k)} && (7)
\end{aligned}
$$

The discretional of BRIAN formula is based on the equation 6 at each of the levels,
i. at the first intermediate level (the $(k+\frac{1}{4})^{th}$ iterate

$$
\begin{aligned}
u_1^{(k+\frac{1}{4})} &= \frac{r_1 u_1^{(k)} - b u_2^{(k)} + f_1}{r_2} \\
u_i^{(k+\frac{1}{4})} &= \frac{E u_{i-1}^{(k)} + F u_i^{(k)} + G u_{i+1}^{(k)} + H u_{i+2}^{(k)} + J_i}{\Delta} \\
u_{i+1}^{(k+\frac{1}{4})} &= \frac{\widetilde{E} u_{i-1}^{(k)} + \widetilde{F} u_i^{(k)} + \widetilde{G} u_{i+1}^{(k)} + \widetilde{H} u_{i+2}^{(k)} + \widetilde{J}_{i+1}}{\Delta} && (8)
\end{aligned}
$$

$$\widetilde{E} = c^2,\ \widetilde{F} = -cr_1,\ \widetilde{G} = r_1r_2,\ \widetilde{J}_{i+1} = -cf_i + r_2f_{i+1}),\quad \widetilde{H} = \begin{cases} 0 & i = m \\ -br_2 & i \neq m \end{cases}$$

ii. at the second intermediate level (the $(k+\frac{1}{2})^{th}$ iterate

$$u^{(k+\frac{1}{2})} = r(rI + \mathbf{G}_2)^{-1}u^{(k+\frac{1}{4})} + (rI + \mathbf{G}_2)^{-1}\mathbf{G}_2u^{(k)}$$

the BRIAN method formula on $(k+\frac{1}{2})^{th}$ is similar to equations (5) by replaced $(k+\frac{1}{4})$ with $(k+\frac{1}{2})$
iii. at the third intermediate level (the $(k+1)^{th}$ iterate

$$u^{(k+1)} = 2u^{(k+\frac{1}{2})} - u^{(k)}$$

There are no communication cost involved in this time step.

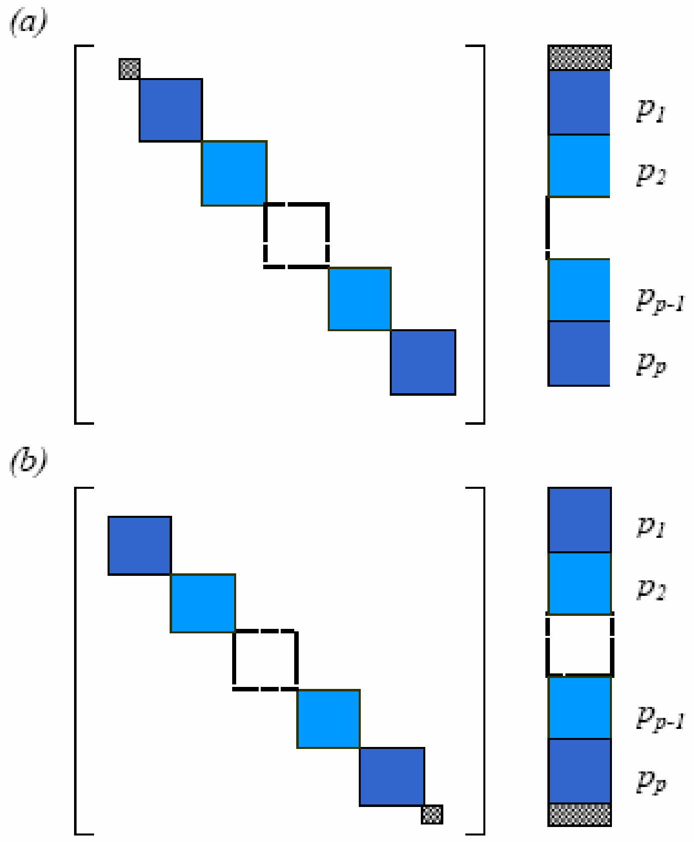

Figure 8: Subdomain is decomposited to processors p in block ordering

The subdomains of BRIAN method are assigned to processors p in block ordering as shown in figure above. As illustrated in figure above, the domain decomposition for BRIAN methods is implemented in two time level. The communications are needed for the computations involved when the next iterations are needed. The parallelization of

BRIAN and AGE is achieved by assigning the explicit block (2x2) in this way and proved that the computations involved are independent. The parallelism strategy is straight forward and the domain is distributed to non-overlapping subdomain. Based on the limited parallelism, this scheme can be effective in reducing computational complexity and data storage accesses in distributed parallel computer systems. The iterative procedure is continued until convergence is reached when the requirement of convergent criterion is met.

3.1.3 Charlie's Method

Charlie's method is an explicit predictor-corrector type algorithm in which the predictor is a transient Euler forward approximation of the differential equation and the corrector is a convex-type operation. It was proposed by Dey and Dey (1983) to solve fluid flow problems. Consider the initial value problem

$$\frac{du}{dt} = f(u); \qquad u(t_0) = u_0, \tag{1}$$

to be approximated by Euler's method

$$U^{m+1} = U^m + \Delta t\, f(U^m), \quad U_0 = u_0. \tag{2}$$

δ is the time step and is U^m the grid function corresponding to $u(t^m)$, $U^m \simeq u(t^m)$.

Charlie's algorithm for solving equation (1) is a two-step procedure

$$\begin{aligned} &\text{predictor:} \quad \hat{U}^m = U^m + \Delta t\, f(U^m) \\ &\text{corrector:} \quad U^{m+1} = (1-\gamma)\hat{U}^m + \gamma[U^m + \Delta t\, f(\hat{U}^m)] \end{aligned} \tag{3}$$

where $0<\gamma<1$. If $\gamma=0$, the original (explicit) method is recovered by the predictor.

As an example of a partial differential equation consider the one-dimensional heat equation

$$\frac{\partial u}{\partial t} = \frac{\partial^2 u}{\partial x^2} \tag{4}$$

with initial condition $u(x,0) = \sin \pi x$ for $0 < x < 1$ and boundary conditions $u(0,t) = u(1,t) = 0$ for all t.

The exact solution is given by

$$u(x,t) = e^{-\pi^2 t} \sin \pi x.$$

The solution of equation (4) by Charlie's method may be obtained by applying the usual explicit FD formula that utilizes a forward Euler step for the time derivative and a central difference replacement for the spatial derivative:

$$\begin{aligned}&\text{predictor:}\quad \hat{U}_i^m = U_i^m + r(U_{i-1}^m - 2U_i^m + U_{i+1}^m), \quad i = 1, 2, \ldots, n\\ &\text{corrector:}\quad U_i^{m+1} = (1-\gamma)\hat{U}_i^m + \gamma\left[U_i^m + r(\hat{U}_{i-1}^m - 2\hat{U}_i^m + \hat{U}_{i+1}^m)\right], \qquad (5)\\ &\qquad\qquad i = 1, 2, \ldots, n\end{aligned}$$

where $U_i^m = U(x_i, t_m)$ is the grid function corresponding to $u(x_i, t_m)$, Δt is the time step, *h* is the spatial mesh size, and $r = \Delta t/h^2$. If $\gamma = 0$, the corrector is not implemented and the algorithm again defaults to the underlying explicit method. Osman and Wood (2001) have shown that the stability property of the method is better than the simple explicit scheme by improving the time step by a factor of 4 from to $\Delta t = h^2/2$ to $\Delta t = 2h^2$. This is achieved when γ = 1/8. They also show that the range of *r* depends on γ as follows:

$$0 < r < \frac{-1 + \sqrt{1 - 8\gamma}}{8\gamma}, \qquad 0 < \gamma < \frac{1}{8}$$

$$0 < r < \frac{1}{4\gamma}, \qquad \frac{1}{8} \le \gamma < 1.$$

Parallel implementation

As Charlie's method is fully explicit, its attractive feature can be exploited for parallelization. The computational domain, consisting of both equations (5), is decomposed into a number of non-overlapping subdomains. A mapping strategy is then used to equivalently assign the subdomains to *p* processors in explicit $(\frac{n}{p} \times \frac{n}{p})$ block ordering independently.

The domain decomposition for the method is implemented in two time levels. The communication activities are required when the next iterations are needed in the case of the convergence criterion is not satisfied. Charlie's method is an effective scheme in reducing computational complexity and data storage accesses on homogeneous PC cluster system.

3.1.4 Gauss-Seidel Method

Gauss-Seidel method is chosen as a control schemes. The Gauss-Seidel method is a technique used to solve a linear system of equations. The method is named after the German mathematicians Carl Friedrich Gauss and Philipp Ludwig von Seidel. The method is similar to the Jacobi method (and likewise diagonal dominance of the system is sufficient to ensure convergence, meaning the method will work).

We seek the solution to a set of linear equations, expressed in matrix terms as

$$A\phi = b.$$

The Gauss-Seidel iteration is

$$\phi^{(k+1)} = (D-L)^{-1}\left(U\phi^{(k)} + b\right),$$

where D, $-L$, and $-U$ represent the diagonal, lower triangular, and upper triangular parts of the coefficient matrix A and k is the iteration count. This matrix expression is mainly of academic interest, and is not used to program the method. Rather, an element-based approach is used:

$$\phi_i^{(k+1)} = \frac{1}{a_{ii}}\left(b_i - \sum_{j<i} a_{ij}\phi_j^{(k+1)} - \sum_{j>i} a_{ij}\phi_j^{(k)}\right),\ i = 1, 2, \ldots, n.$$

Note that the computation of $\phi_i^{(k+1)}$ uses only those elements of $\phi^{(k+1)}$ that have already been computed and only those elements of $\phi^{(k)}$ that have yet to be advanced to iteration $k + 1$. This means that no additional storage is required, and the computation can be done in place ($\phi^{(k+1)}$ replaces ($\phi^{(k)}$). While this might seem like a rather minor concern, for large systems it is unlikely that every iteration can be stored. Thus, unlike the Jacobi method, we do not have to do any vector copying should we wish to use only one storage vector. The iteration is generally continued until the changes made by an iteration are below some tolerance.

Algorithm

```
Chose an initial guess $\varphi^0$
for k := 1 step 1 until convergence do
for i := 1 step until n do
$\sigma = 0$
for j := 1 step until i-1 do
$\sigma = \sigma + a_{ij}\phi_j^{(k)}$
end (j-loop)
for j := i+1 step until n do
$\sigma = \sigma + a_{ij}\phi_j^{(k-1)}$
end (j-loop)
$\phi_i^{(k)} = \frac{(b_i - \sigma)}{a_{ii}}$
end (i-loop)
check if convergence is reached
end (k-loop)
```

3.2 Model Problems

The model problem under consideration is one dimensional parabolic equation (Smith, 1979).

$$\frac{\partial U}{\partial t} = \frac{\partial^2 U}{\partial x^2}, \quad 0 \le x \le 1, \quad 0 < t, \tag{0.0.1}$$

Equation 0.0.1 is discretized by the finite difference formula and leads to the generalized approximation stencil as,

$$\begin{aligned} -\lambda\theta u_{i-1,j+1} + (1+2\lambda\theta)u_{i,j+1} - \lambda\theta u_{i+1,j+1} &= \lambda(1-\theta)u_{i-1,j} + [1-2\lambda(1-\theta)]u_{i,j} \\ &+ \lambda(1-\theta)u_{i+1,j} \qquad (0.0.2) \end{aligned} \quad 1$$

where $i = 1, 2, 3, ..., m$, $j = 1, 2, 3, ..., T$ and $\lambda = \frac{\Delta t}{(\Delta x)^2}$ leads to the a large and sparse linear system of equation,

$$\mathbf{A}u = \mathbf{f} \tag{0.0.3}$$

The parallel iteration algorithms for solving a large and sparse linear system 0.0.3 has been developed and implemented successfully by Alternating Group Explicit Method (AGE), Alternating Group Explicit-Conjugate Gradient Method (AGE_CG), Gauss Seidel Red Black Method (GSRB) and Gauss Seidel Red Black-Conjugate Gradient Method (GSRB_CG)

3.3 Implementation on Message Passing Systems

Message passing is referred as:

1. Objects communicate by sending messages.
2. Messages convey some form of information.
3. An object requests another object to carry out an activity by sending it a message.
4. Most messages pass arguments back and forth.
5. Meilir Page-Jones defines three types of messages:

    i. Informative - send information for the object to update itself.
    ii. Interrogative - ask an object to reveal some information about itself
    iii. Imperative - take some action on itself, or another object

6. Grady Booch defines four types of messages:

    i. Synchronous - receiving object starts only when it receives a message from a sender, and it is ready.
    ii. Balking - sending object gives up on the message if the receiving object is not ready to accept it.
    iii. Timeout - sending object waits only for a certain time period for the receiving object to be ready to accept the message.
    iv. Asynchronous - sender can send a message to a receiver regardless of whether the receiver is ready to receive it.

The world's largest supercomputers are used almost exclusively to run applications which are parallelized using Message Passing. Parallel programming by definition involves co-operation between processes to solve a common task. The programmer has to define the tasks that will be executed by the processors, and also how these tasks are to synchronize and exchange data with one another. In the message-passing model the tasks are separate processes that communicate and synchronize by explicitly sending each other message. All these parallel operations are performed via calls to some message-passing interface that is entirely responsible for interfacing with the physical communication network linking the actual processors together.

Message Passing Systems referred as:

1. Processors communicate by sending messages over bidirectional communication channels
2. Pattern of connections describes the topology of the system
3. Topology represented by undirected graph
4. nodes - processors
5. edges - channels between processors
6. Collection of channels is called the network
7. Processor's local program enables
   i. local computation
   ii. sending messages to and receiving messages from each of the neighbors

Synchronous Systems referred as:

1. Processors execute in lock-step
2. The sequence of alternating configurations and events is partitioned into disjoint rounds
3. A round consists of a deliver event for every message in an outbuf variable until all outbuf variables are empty, and then one computation event for every processor

That is, a round consists of delivering all pending messages and then having every processor take an internal computation step to process all delivered messages:

1. An execution is admissible if it is infinite
2. Because of the round structure, this implies that every processor takes an infinite number of computation steps and every message sent is eventually delivered in a synchronous system with no failures, once the algorithm is fixed, there can be only one execution for each initial configuration. This is not true in asynchronous systems due to interleaving of the processor steps and the message delays being not fixed.

As the AGE method is fully explicit, its feature can be fully utilized for parallelization. Firstly, Domain Ω is distributed to Ω^p subdomains by the master processor. The partitioning is based on domain decomposition technique. Secondly, the subdomains Ω^p of AGE method are assigned into p processors in block. The communication activities between the slave processors are needed for the computations in the next iterations. The parallelization of AGEB is achieved by assigning the explicit *(2x2)* block systems. The parallelism strategy is straightforward with no overlapping subdomains. Based on the limited parallelism, this scheme can be effective in reducing computational complexity and data storage accesses in distributed parallel computer systems.

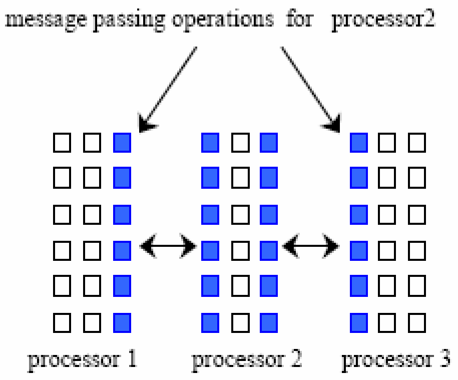

Figure 9: Message passing operations between processors

The parallel strategies are based on the non-overlapping subdomain. There are no data exchange between the neighboring processors at the iteration *(k)* but there are inter-processor communications between the iteration *(k)* and the next iteration *(k+1)*. A typical parallel implementation of a parallel AGE_CG assigns several mesh points to each processor p such that each processor only communicates with its two nearest neighbors; see figure above, where there are $p=3$ and grids $m=54$. The computations of the approximation solutions in subdomain are executed independently for every time level. Iterate each group tasks in the following order, where it is indicates the synchronization points take the place and each task is assigned into one processor.

$$x_0, x_1, x_2, \ldots, x_{26} // x_{27}, x_{28}, x_{29}, \ldots, x_{53} // x_{54}, x_{55}, x_{56}, \ldots, x_{80}$$

Table 3: Computational complexity and communication cost for the parallel algorithms

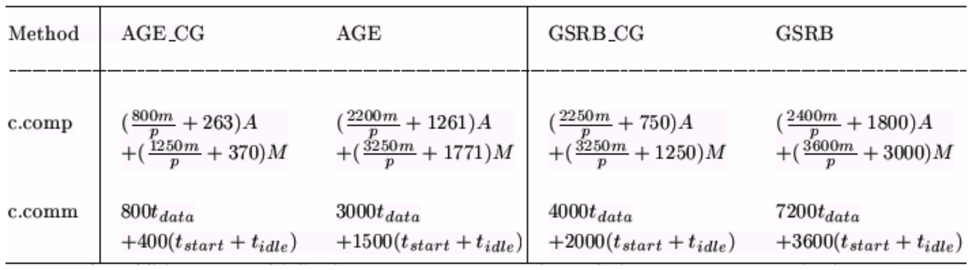

Method	AGE_CG	AGE	GSRB_CG	GSRB
c.comp	$(\frac{800m}{p}+263)A$ $+(\frac{1250m}{p}+370)M$	$(\frac{2200m}{p}+1261)A$ $+(\frac{3250m}{p}+1771)M$	$(\frac{2250m}{p}+750)A$ $+(\frac{3250m}{p}+1250)M$	$(\frac{2400m}{p}+1800)A$ $+(\frac{3600m}{p}+3000)M$
c.comm	$800t_{data}$ $+400(t_{start}+t_{idle})$	$3000t_{data}$ $+1500(t_{start}+t_{idle})$	$4000t_{data}$ $+2000(t_{start}+t_{idle})$	$7200t_{data}$ $+3600(t_{start}+t_{idle})$

3.4 Parallel Procedure

Implement as an SPMD model

1 The entire array is partitioned and distributed as subarrays to all tasks. Each task owns a portion of the total array.

2 Determine data dependencies

i. Interior elements belonging to a task are independent of other tasks

ii. Border elements are dependent upon a neighbor task's data, necessitating communication.

3 Master process sends initial info to workers, checks for convergence and collects results

4 Worker process calculates solution, communicating as necessary with neighbor processes

5 Pseudo code solution: **red** highlights changes for parallelism.

```
find out if I am MASTER or WORKER

if I am MASTER
  initialize array
  send each WORKER starting info and subarray

  do until all WORKERS converge
    gather from all WORKERS convergence data
    broadcast to all WORKERS convergence signal
  end do

  receive results from each WORKER

else if I am WORKER
  receive from MASTER starting info and subarray

  do until solution converged
    update time
    send neighbors my border info
    receive from neighbors their border info

    update my portion of solution array

    determine if my solution has converged
      send MASTER convergence data
      receive from MASTER convergence signal
  end do

  send MASTER results

endif
```

3.5 Parallel Execution Time and Communication Time

The following definitions are used to measure the parallel strategies, speedup $S_p = \frac{T_1}{T_p}$, efficiency $C_p = \frac{S_p}{P}$, effectiveness $F_p = \frac{C_p}{T_p}$, and temporal performance $L_p = T_p^{-1}$, where T_1 is the execution time on one processor, T_p is the execution time on *p* processors and the unit of L_p is work done per microsecond. The important factors effecting the performance in message-passing on distributed memory computer systems are communication patterns and computational per communication ratios. The important factors effecting the performance in message-passing paradigm on a distributed memory computer systems are communication patterns and computational/ communication ratios. The communication time will depend on many factors including network structure and network contention (Wolfgang, 1988). Parallel execution time, t_{para} is composed of two parts, computation time (t_{comp}) and communication time (t_{comm}). t_{comp} is the time to compute the arithmetic operations such as multiplication and addition operations of a sequential algorithms. Analysis of the t_{comp} assumes that all the processors are the same and the operating at the same speed. t_{comm} will depend upon the size of message. If the number of iterations b, and size of the message for communication m, the formula for communication time is as follows,

$$t_{comm} = b(t_{start} + m\, t_{data} + t_{idle})$$

where t_{start} is the startup time (message latency). t_{data} is time to send a message with no data. The term t_{data} is the transmission time to send one data word. t_{idle} is the time for message latency, time to wait for all the processors to complete the process as shown in the figure below. It is also a means of quantifying the degree of load imbalance in the parallel algorithm. In order to estimate the coefficients t_{start} and t_{data} , a number of experiments were conducted for different message sizes. Table 1 shows that the implementation of CG made the computational complexity and communication cost of AGE and GSRB are decreased.

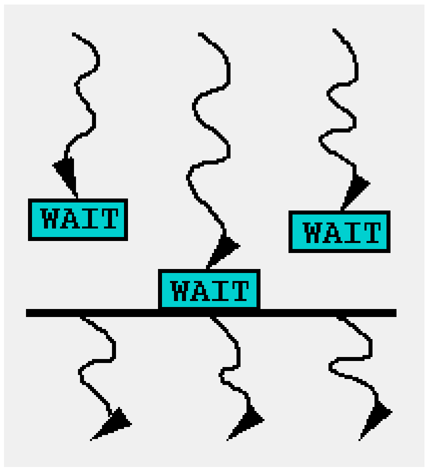

Figure 10: Synchronization of *n* processes. WAIT blocks until all *n* processes have reached barrier.

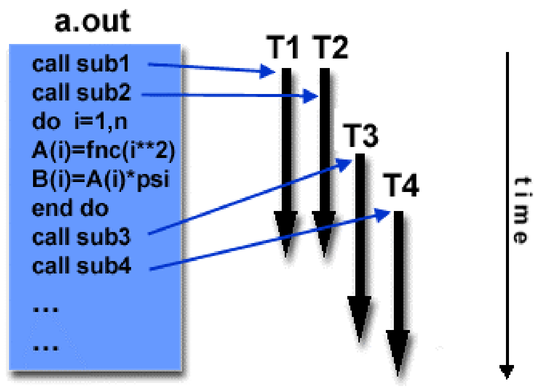

3.5.1 Threads Model

1 In the threads model of parallel programming, a single process can have multiple, concurrent execution paths.

2 Perhaps the most simple analogy that can be used to describe threads is the concept of a single program that includes a number of subroutines:

i. The main program **a.out** is scheduled to run by the native operating system. a.out loads and acquires all of the necessary system and user resources to run.

ii. a.out performs some serial work, and then creates a number of tasks (threads) that can be scheduled and run by the operating system concurrently.

iii. Each thread has local data, but also, shares the entire resources of a.out. This saves the overhead associated with replicating a program's resources for each thread. Each thread also benefits from a global memory view because it shares the memory space of a.out.

iv. A thread's work may best be described as a subroutine within the main program. Any thread can execute any subroutine at the same time as other threads.

v. Threads communicate with each other through global memory (updating address locations). This requires synchronization constructs to insure that more than one thread is not updating the same global address at any time.

vi. Threads can come and go, but a.out remains present to provide the necessary shared resources until the application has completed.

3.5.2 Complexity Measures

1 Worst-Case and Expected-Case Performance
2 Assume each processor's state set includes a subset of terminated states:
3 each processor's transition function maps terminated states only to terminated states:

   i. The system (algorithms) has terminated when all the processors are in terminated states and no messages are in transit.

4 The Message Complexity of an algorithm for both synchronous and asynchronous system is the maximum, over all admissible executions of the algorithm, of the total number of messages sent
5 The Time Complexity of an algorithm for a synchronous message passing system is the maximum number of rounds, in any admissible execution of the algorithm, until the algorithm has terminated
6 In asynchronous systems,

   i. assume that the maximum message delay in any execution is one unit of time and then calculate the running time until termination

7 Timed execution concept

3.5.3 Timed Execution

1 A non negative real number is associated with each event - this is the time at which that event occurs
2 times start at 0

   i. must be non decreasing
   ii. strictly increasing for each individual processor
   iii. must increase without bound if the execution is infinite

3 events in the execution are ordered according to the times they occur

4 several events can happen at the same time as long as they do not occur at the sam processor

5 only finitely many events before a finite time

6 The delay of a message is the time that elapses between the computation event that sends the message and the computation event that processes that message

7 that is, the amount of time the message waits in the sender's outbuf, plus the amount of time the message waits in the recipient's inbuf

8 The Time Complexity of an asynchronous algorithm is the maximum time until termination among all timed admissible execution in which every message delay is at most one.

3.6 Numerical Model

This section describes the development of mathematical modeling and simulation of a one-dimensional thermal EFW model. We developed a sequence of models of increasing refinement. The final model is expected to roughly mimic the actual EFW process. An essential element for the model is that a hot wire acts as a heat source, driving the heat from the fitting, across the air gap, and eventually to the pipe. Temperature distribution in the pipe-fitting is governed by the transient heat conduction equation, in a radial coordinate system, which forms the basis of the heat transfer model. Figure 11 displays a radial cross-section of the pipe-fitting length.

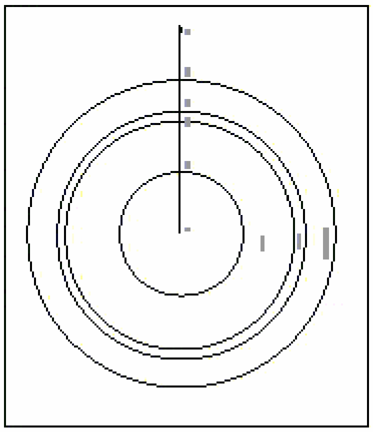

Figure 11: Cross section of pipe-fitting

3.6.1 Fitting Model

Heat transfer in the fitting is induced by an embedded hot wire. For a 1-D radial model, the wire is taken to be one of the nodes located sufficiently close to the inner fitting surface. The appropriate physical heat equation governing the heat transfer process in the fitting is

$$\frac{\partial T_f}{\partial \tau} = \kappa_f \left(\frac{\partial^2 T_f}{\partial R^2} + \frac{1}{R}\frac{\partial T_f}{\partial R} \right), \quad R_I \le R \le R_O, \ \tau \ge 0$$

where $\kappa_f = \lambda_f / \rho_f c_f$. T_{max} is the maximum temperature of the wire and T_∞ is the ambient temperature. Figure 12 shows the evolving of the wire temperature during a heating period of 220 s.

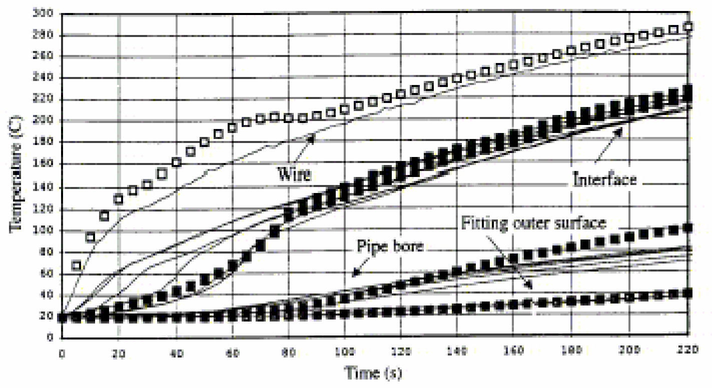

Figure 12: Wire temperature (Wood et. al, 1998)

Based on Figure 12 it is quite reasonable to describe and approximate the wire temperature as a function of time,

$$T_W = \left(\frac{T_{max} - T_\infty}{15} \right) \sqrt{\tau} + T_\infty, \quad 0 \le \tau \le 220.$$

For the thermal boundary conditions, we have assumed the inner and outer fitting surface is losing heat to the ambient by convection given by

$$h_I (T_f - T_\infty) = -\lambda_f \frac{\partial T_f}{\partial R} \quad \text{at } R = R_I$$

$$-\lambda_f \frac{\partial T_f}{\partial R} = h_O (T_f - T_\infty) \quad \text{at } R = R_O.$$

Defining the dimensionless variables

$$U_f = \frac{T_f - T_\infty}{T_{max} - T_\infty}, \quad t = \frac{\kappa_f \tau}{R_O^2}, \quad r = \frac{R}{R_O},$$

the physical equations reduce to

$$\frac{\partial U_f}{\partial t} = \frac{\partial^2 U_f}{\partial r^2} + \frac{1}{r}\frac{\partial U_f}{\partial r}, \quad r_I \le r \le 1,\ t \ge 0$$

with wire temperature function

$$U_f = \frac{1}{15}\sqrt{\omega t}, \quad \text{where } \omega = \frac{R_O^2}{\kappa_f} \text{ at } r = r_W,$$

and boundary conditions

$$\beta_I U_f = \frac{\partial U_f}{\partial r}, \quad \text{where } \beta_I = \frac{h_I R_O}{\lambda_f} \text{ at } r = r_I,$$
$$\frac{\partial U_f}{\partial r} = \beta_O U_f, \quad \text{where } \beta_O = \frac{-h_O R_O}{\lambda_f} \text{ at } r = 1.$$

3.6.2 Pipe Model

Next, we add the pipe `problem' to the existing fitting model by assuming a perfect thermal contact (no thermal resistance) at the pipe-fitting interface. The heat equation in the pipe is the same as in the fitting (with different thermal diffusivity). Thus,

$$\frac{\partial T_p}{\partial \tau} = \kappa_p \left(\frac{\partial^2 T_p}{\partial R^2} + \frac{1}{R}\frac{\partial T_p}{\partial R} \right), \quad R_b \le R \le R_g,\ \tau \ge 0.$$

Thermal modelling at the interface accounting for perfect contact is

$$\lambda_p \frac{\partial T_p}{\partial R} = \lambda_f \frac{\partial T_f}{\partial R} \quad \text{at } R = R_g = R_I,$$

while the inner pipe surface loses heat to the ambient through convection given by

$$h_b(T_\infty - T_p) = -\lambda_p \frac{\partial T_p}{\partial R} \quad \text{at } R = R_b.$$

The pipe physical variables are nondimensionalized with respect to the same parameters as in the fitting, giving

$$\frac{\partial U_p}{\partial t} = \varphi_p \left(\frac{\partial^2 U_p}{\partial r^2} + \frac{1}{r} \frac{\partial U_p}{\partial r} \right), \quad r_b \le r \le r_g,\ t \ge 0$$

where $\varphi_p = \kappa_p / \kappa_f$. Boundary conditions respectively becomes

$$\frac{\partial U_p}{\partial r} = \lambda \frac{\partial U_f}{\partial r}, \quad \text{where } \lambda = \frac{\lambda_f}{\lambda_p} \text{ at } r = r_g,$$

$$\frac{\partial U_p}{\partial r} = \beta_b U_p, \quad \text{where } \beta_b = \frac{h_b R_O}{\lambda_p} \text{ at } r = r_b.$$

3.6.3 Fixed Gap Model

The next stage of the modelling is to include a fixed gap between the pipe and fitting. We have considered two types of thermal model across the gap: convection alone, and convection plus radiation heat transfer expression. Conduction in the gap is not considered since the thermal conductivity of air is very low, making the flow of heat very slow. The governing equations in the pipe and fitting stay the same, as do the boundary condition at the inner pipe surface and outer fitting surface. Figure 13 illustrates the heat transfer process in the pipe-gap-fitting during the heating up period.

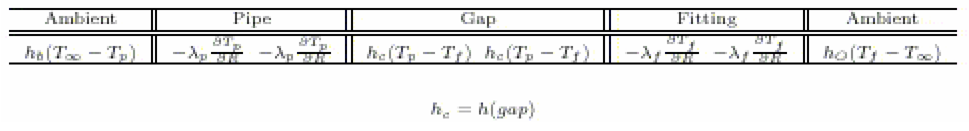

Ambient	Pipe	Gap	Fitting	Ambient
$h_b(T_\infty - T_p)$	$-\lambda_p \frac{\partial T_p}{\partial R}$ $-\lambda_p \frac{\partial T_p}{\partial R}$	$h_c(T_p - T_f)$ $h_c(T_p - T_f)$	$-\lambda_f \frac{\partial T_f}{\partial R}$ $-\lambda_f \frac{\partial T_f}{\partial R}$	$h_O(T_f - T_\infty)$

$h_c = h(gap)$

Figure 13: Heat Transfer Process

As for the dimensionless form of the model, only the boundary conditions at the pipe-fitting interface need to be considered (the others are kept unchanged).

Chapter 4

Computational Results

4.1 AGE and Brian Methods

The experiments were run on the homogeneous cluster of 20 Intel Pentium IV PCs, each with storage of 20GB and speed of 1.6 MHz.

Numerical experiments on a heat conduction problem in equation (1) confirmed the viability of the sequential algorithm of AGE_CG method. While the convergence and accuracy of the results are comparable to the existing methods (i.e. AGE, GSRB_CG and GSRB), see Table 4. Due to the implementation of CG, the number of iterations of AGE_CG and GSRB_CG are less AGE and GSRB. The sequential AGE_CG is better in convergence than GSRB_CG. The results also show that the time execution for AGE_CG and GSRB_CG was about 39% and 35% shorter than AGE and GSRB. Furthermore, AGE_CG is the best in terms of convergence and accuracy. The adaptation CG method into the sequential AGE, make the convergence of AGE_CG increasing to 80% and the computational complexity decreasing to 64.77%.

Table 4: Performance measurements of the sequential AGE_CG, AGE, GSRB_CG

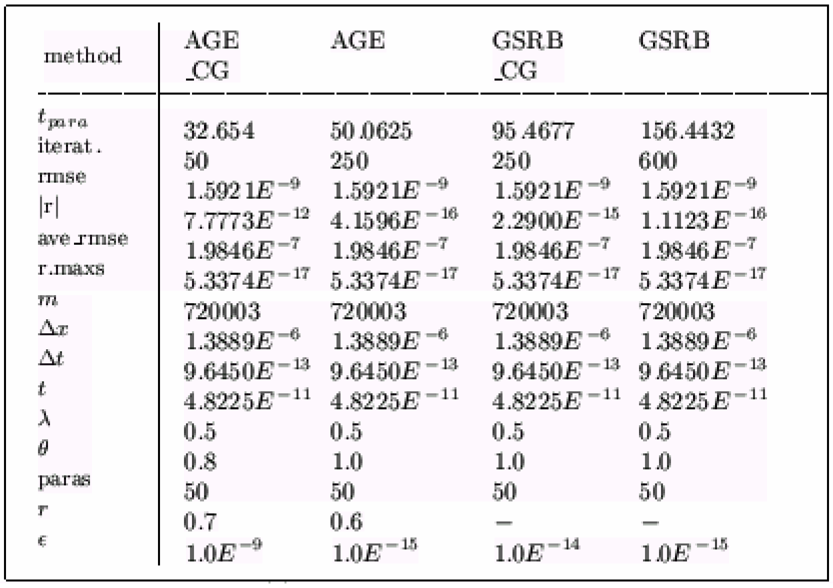

method	AGE _CG	AGE	GSRB _CG	GSRB
t_{para}	32.654	50.0625	95.4677	156.4432
iterat.	50	250	250	600
rmse	$1.5921E^{-9}$	$1.5921E^{-9}$	$1.5921E^{-9}$	$1.5921E^{-9}$
$\|r\|$	$7.7773E^{-12}$	$4.1596E^{-16}$	$2.2900E^{-15}$	$1.1123E^{-16}$
ave_rmse	$1.9846E^{-7}$	$1.9846E^{-7}$	$1.9846E^{-7}$	$1.9846E^{-7}$
r_maxs	$5.3374E^{-17}$	$5.3374E^{-17}$	$5.3374E^{-17}$	$5.3374E^{-17}$
m	720003	720003	720003	720003
Δx	$1.3889E^{-6}$	$1.3889E^{-6}$	$1.3889E^{-6}$	$1.3889E^{-6}$
Δt	$9.6450E^{-13}$	$9.6450E^{-13}$	$9.6450E^{-13}$	$9.6450E^{-13}$
t	$4.8225E^{-11}$	$4.8225E^{-11}$	$4.8225E^{-11}$	$4.8225E^{-11}$
λ	0.5	0.5	0.5	0.5
θ	0.8	1.0	1.0	1.0
paras	50	50	50	50
r	0.7	0.6	–	–
ϵ	$1.0E^{-9}$	$1.0E^{-15}$	$1.0E^{-14}$	$1.0E^{-15}$

This section presents the numerical properties of the parallel solver on the homogeneous architecture of 20 PCs with Linux operating, Intel Pentium IV processors, 20GB HDD, connected with internal network Intel 10/100 NIC and using message-passing libraries, PVM. The following definitions are used to measure the parallel algorithms, speedup $S_p=T_1/T_p$ efficiency $C_p=S_p/p$ effectiveness $F_p= S_p/C_p$ and temporal performance $L_p=1/T_p.$ Where T_1 is the execution time on one processor, T_p is the execution time on p processors. Parallel algorithm of Gauss Seidel Red Black is chosen as the control scheme. The graph of the speedup, efficiency and effectiveness versus number of the processors were plotted in Figures 14 below. The parallel algorithm with the highest performance executed in the least time and is therefore the best algorithm.

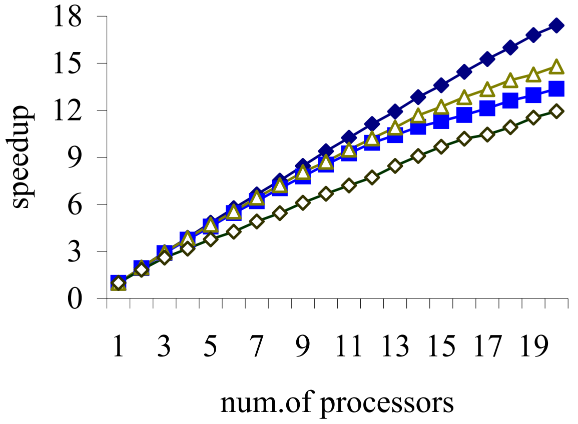

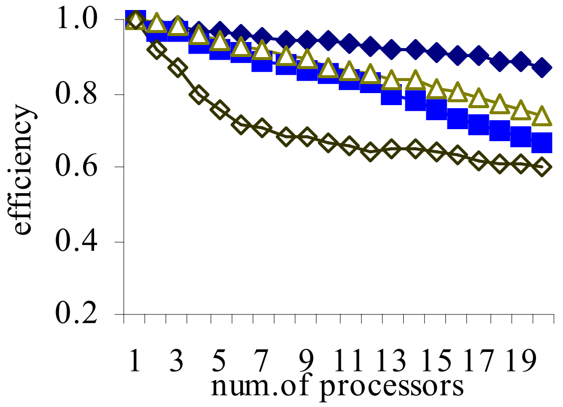

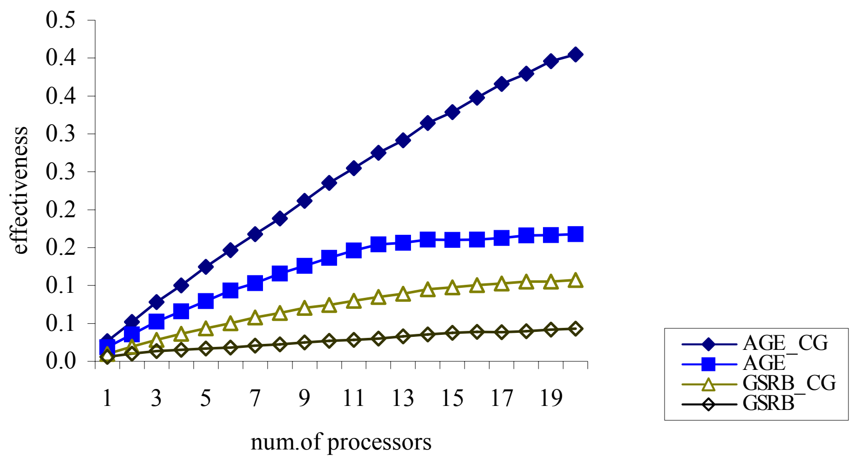

Figure 14: The parallel performances vs. number of processors

Table 5: The gain of communication time, computational complexity and t_{comp}/t_{comm} ratio versus number of processors

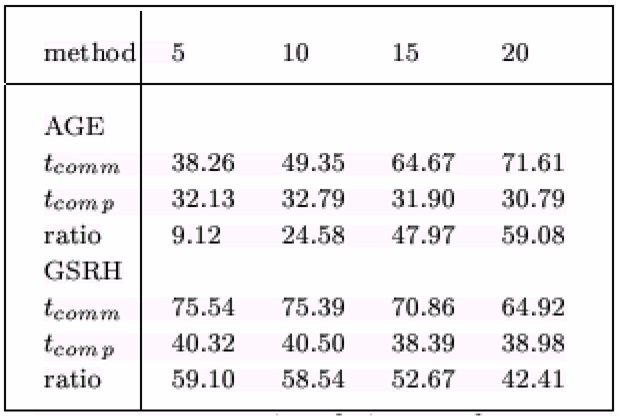

method	5	10	15	20
AGE				
t_{comm}	38.26	49.35	64.67	71.61
t_{comp}	32.13	32.79	31.90	30.79
ratio	9.12	24.58	47.97	59.08
GSRH				
t_{comm}	75.54	75.39	70.86	64.92
t_{comp}	40.32	40.50	38.39	38.98
ratio	59.10	58.54	52.67	42.41

As expected, the execution time decreases with the increasing *p*. AGE_CG strategy is faster than other parallel algorithms for any number of processors. The implementation of CG on AGE and GSRB are found the best performance because of the minimum memory access and data sharing between processors. All the parallel strategies of AGE_CG yield approximately equal performance in speedup. The efficiency of AGE and GSRB are decreased drastically as compared to AGE_CG and GSRB_CG. Due to this result, the additional overhead imposed by having communications routed though the PVM daemon. The communication cost of AGE_CG is decreasing to 73.33%. From Figure 14, the results have shown that the effectiveness of AGE_CG is superior than AGE, GSRB_CG and GSRB for all numbers of processors. It is indicated that the superiority of the AGE_CG method lies in its temporal performance.

4.2 Performance of Charlie's Method

The results of parallel performance are shown in figure 15-19. Referring to figure 15, the execution time of Charlie's method decreases faster than GSRB when the number of processors increases. The speedup, effectiveness, and temporal performance graphs indicate that the parallelism of Charlie's method is highly encouraging compared to GRSB as shown in figures 16,17 and 18.

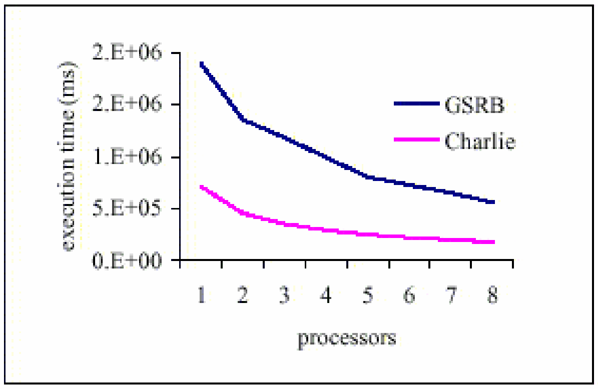

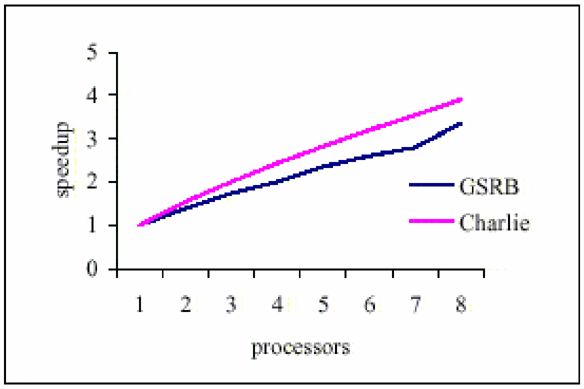

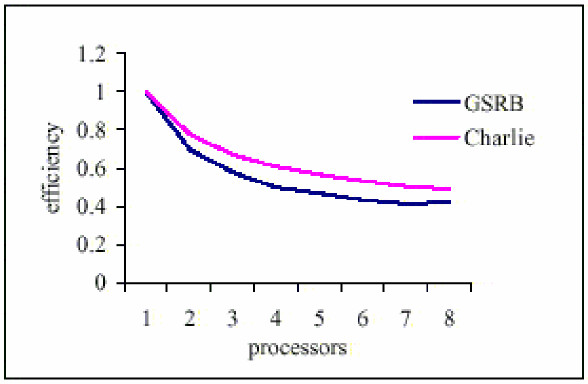

Figure 15-17: Efficiency vs number of processors

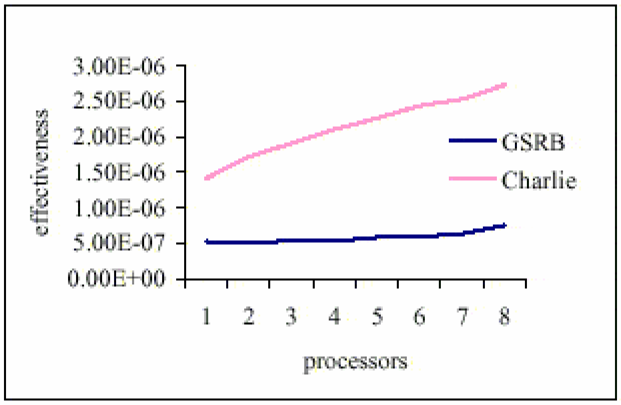

Figure 18: Effectiveness vs number of processors

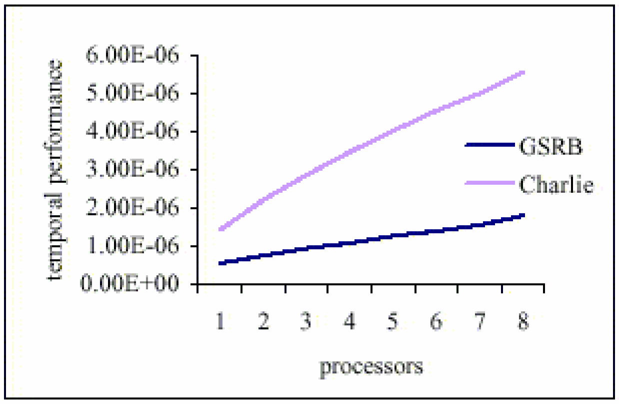

Figure 19: Temporal performance vs number of processors

Further, Charlie's scheme is more efficient compared to GSRB as illustrated in figure 20. The graph of the scheme decreases slowly when the number of processors increases. This is because Charlie's scheme uses minimum communication, idle and startup time. These phenomena come from the fact that the scheme utilizes minimum number of iterations to fulfill the convergence criterion requirement.

Another nice feature of Charlie's method is that it also allows for inconsistencies due to imbalance load balancing when the extra computation cost is needed. It is to be noted that the method does not require any specific strategy in the transition process from sequential to parallel algorithm compared to other explicit iterative methods such as IADE and EDG .

Charlie's scheme demonstrates favourable outcomes with respect to sequential performance measurements as well. Figure 1 presents the performance based on the number of iterations, the root mean square error (rmse), the maximum rmse, the absolute maximum relative error and the execution time.

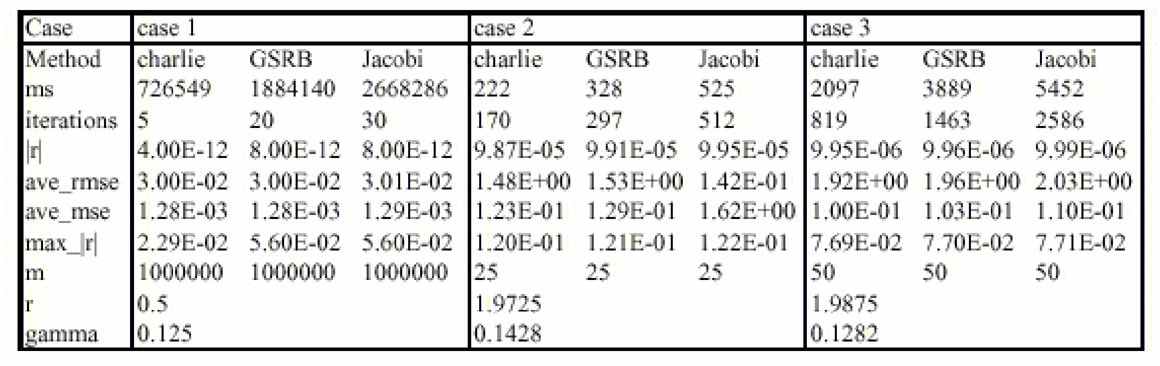

Case	case 1			case 2			case 3		
Method	charlie	GSRB	Jacobi	charlie	GSRB	Jacobi	charlie	GSRB	Jacobi
ms	726549	1884140	2668286	222	328	525	2097	3889	5452
iterations	5	20	30	170	297	512	819	1463	2586
|r|	4.00E-12	8.00E-12	8.00E-12	9.87E-05	9.91E-05	9.95E-05	9.95E-06	9.96E-06	9.99E-06
ave_rmse	3.00E-02	3.00E-02	3.01E-02	1.48E+00	1.53E+00	1.42E-01	1.92E+00	1.96E+00	2.03E+00
ave_mse	1.28E-03	1.28E-03	1.29E-03	1.23E-01	1.29E-01	1.62E+00	1.00E-01	1.03E-01	1.10E-01
max_|r|	2.29E-02	5.60E-02	5.60E-02	1.20E-01	1.21E-01	1.22E-01	7.69E-02	7.70E-02	7.71E-02
m	1000000	1000000	1000000	25	25	25	50	50	50
r	0.5			1.9725			1.9875		
gamma	0.125			0.1428			0.1282		

Figure 20: Sequential performance measurement

The rate of convergence and the accuracy of the scheme are much superior than that of GSRB and Jacobi. For large scale problems such as in case 1, the relative percentage of accuracy, rate of convergence and execution time are respectively 50%, 75% and 61% better than GSRB.

4.3 Fitting Result

With uniform grids and a wire depth of 1mm (from the inner fitting), the simulated temperature profile in the fitting during the heating period (of 220s) is displayed in Figure 21. The peak in the profile represents the wire temperature. A stable time step *k* is obtained through an heuristic approach, given by min $\{k_1, k_2, k_3\}$ where

$$\begin{aligned} k_1 &= \frac{(s_2^2 - s_1^2)h_1}{2(s_2 + s_1 h_1 \beta_I)}, \\ k_2 &= \min\left\{\frac{(s_{i+1}^2 - s_i^2)h_i h_{i-1}}{2(s_{i+1}h_{i-1} + s_i h_i)}\right\}, \quad i = 2, \ldots, n \\ k_3 &= \frac{(s_{n+2}^2 - s_{n+1}^2)h_n}{2(s_{n+1} - s_{n+2}h_n \beta_O)}. \end{aligned}$$

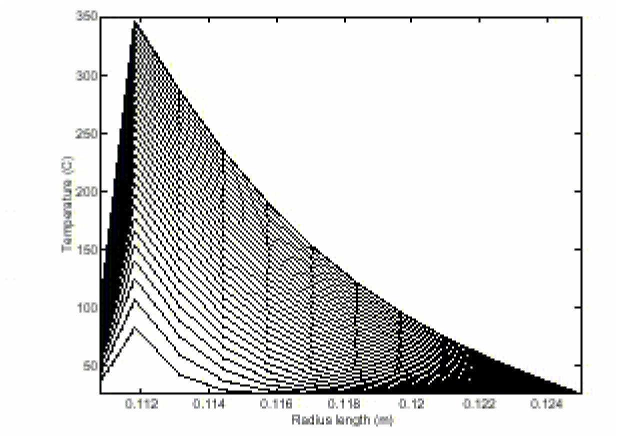

Figure 21: Temperature profile in fitting

4.4 Pipe Result

Figure 22 shows the temperature profile in the pipe and fitting. The assumption of perfect thermal contact at the interface ensures temperature continuity as clearly seen from the graphs. However, there is a jump in the temperature gradients because of the different thermal conductivities (Figure 22a). If they were the same, we would anticipate a smooth gradient at the interface (Figure 22b).

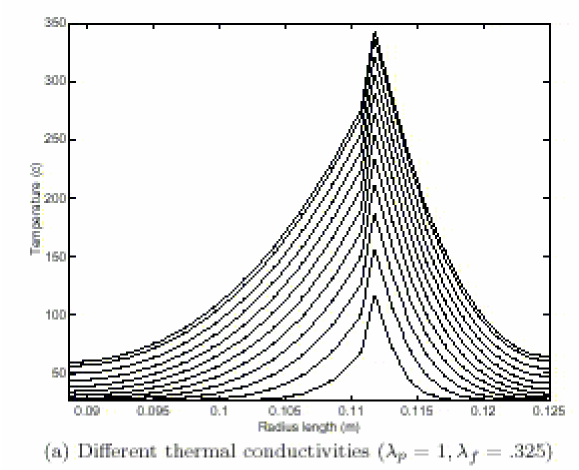

(a) Different thermal conductivities ($\lambda_p = 1, \lambda_f = .325$)

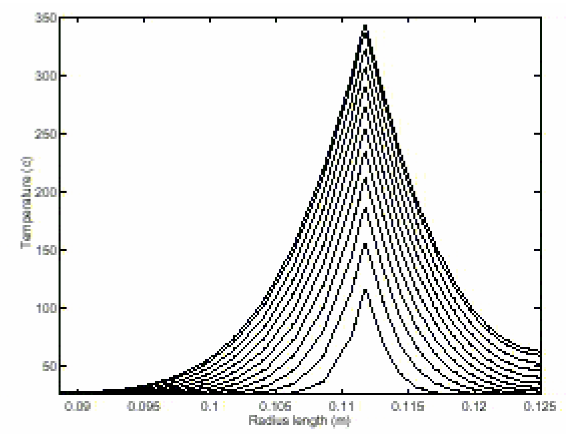

(b) Same thermal conductivities ($\lambda_p = \lambda_f = .325$)

Figure 22: Temperature profile in pipe-fitting

A stable time step is obtained through the same heuristic argument as before, where *k* is now the minimum time step considered at the inner pipe surface, pipe-fitting interface, and the outer fitting surface.

Chapter 5

Concluding Remarks and Suggestions

Compared to AGE_CG, AGE, GSRB_RB and GSRB methods, sending a larger value of messages and the frequency of communications are reflected the communication time. Therefore, the cost communication and computational complexity are effected the speedup ratio, efficiency and effectiveness of the parallel algorithms. Table 2 shows that the gain in communication time and t_{comp}/t_{comm} ratio of AGE method is lower than GSRB methods. The gains in ratio are implied that the computational complexity of the algorithms which clearly shows that the AGE_CG method has less memory accesses than AGE method with the limited communication time.

The result on a cluster of workstations shows that AGE_CG method is the most superior and effective method among the three algorithms. Parallel CG method is inherently explicit, the domain decomposition strategy is efficiently utilized and straightforward to implement on a cluster of workstations. In the context communication activities and work balance on a distributed parallel computer systems, we reach the conclusion that AGE_CG and GSRB_CG methods are alternative to AGE and GSRB.

With regard to Charlie’s method, our experiment shows that with suitable choice of filtering parameter γ Charlie's method has the potential to be a favourite scheme for solving parabolic problems. We have demonstrated that the method is very attractive to solving large scale linear heat transfer problems because of its simplicity and high performance achievements. Further research is underway to compare the performance with other well known classes iterative methods of IADE, AGE and EDG .

As for the electrofusion jointing process simulation, we managed to run the model based on explicit scheme only. The temperature profile describing thermal behaviour in the pipe-fitting showed that the simulation models are correct. Numerical experiments incorporating Charlie’s method for the electrofusion process simulation will be carried in the near future.

REFERENCES

Alias, Sahimi., Abdullah, A. 2002.Proceedings of the 7th Asian Technology Conference in Mathematics 7:390-97

Al Geist, A. Beguelin, J. Dongarra, W. Jiang, R. Manchek,V. Sunderam, PVM : Parallel Virtual Machine, A Users' Guide and Tutorial for Networked Parallel Computing. MIT Press, Cambridge, Mass, 1994

D.J. Evans, M.S. Sahimi. 1989, The alternating Group Explicit Iterative method (AGE) to Solve Parabolic and Hyperbolic Partial Differential Equation. *In Annual Review of Numerical Fluid Mechanics and Heat Transfer,*Vol.2,pp.283-389, Hemisphere Publication Corp. New York.

Wolfgang, S.P. 1994. The Logical Design of Parallel Operating Systems. New Jersey: PTR Prentice Hall.

Abdullah, A.R. 1991a. The Four Point Explicit Decoupled Group (EDG) Method: A Fast Poisson Solver. Inter. Journal Computer mathematics.
38 61--70.

Alias, N., Sahimi, M.S. Abdullah, A.R. 2002. Parallel Algorithms On Some Numerical Techniques Using PVM Platform On A Cluster Of workstations. Proc. of The 7 Asian Technology Conference in Mathematics. 7: 390--97.

Sahimi, M.S. Alias, N. 2001. Beberapa Strategi Selari Kaedah Tak Tersirat Penghuraian Berselang-Seli Ke Atas Mesin Maya Selari. Pros. Simposium Kebangsaan Sains Matematik ke-9. : 284--288.

Alias, N., Sahimi, M.S. Abdulllah, A.~R. 2002. The Parallel Implementation of IADE and AGE Algorithms Using Parallel Virtual Machine On A Distributed Parallel Systems. Proc. of The Conference On Information Technology Research Application.7 390--97.

Evans, D.J. Sahimi, M.S. 1989. The alternating Group Explicit (AGE) Iterative method for Solving Parabolic Equations II: 3 Space Dimensional Problems. International Journal Computer Mathematic 26: 117--142.

J.~Bowman (1997). A review of the electrofusion joining process for polyethylene pipe systems, \emph{Polym. Eng. Sci.}, 37,674-691.

G.F.~Rosala (1995). The Process Mechanics of Polymer Pipes Welding by Electrofusion, Ph.D. Thesis, University of Bradford, UK.

J.~Bowman, T.~Medhurst and R.~Portas (1992). Procedures for quantifying the strength of electrofusion joints, \Proc. Plastics Pipes VIII, Koningshof, The Netherlands, B2/5.1-12.

J.Bowman (1991). Fusion joining of cross-linked polyethylene pipe, in Advances in joining plastics and composites, TWI paper 13, Bradford, UK.

D.Morris and B.W.~Gill (1992). Fusion jointing of PE pipes - a water industry perspective, Proceedings of Plastics Pipes VIII, Koningshof, Netherlands. B2/1-8.
P.E.O'Donoghue, M.F.Kanninen, S.T.Green and S.C.Grigory (1991). Results of a thermomechanical analysis model for electrofusion joining of PE gas pipes, Proceedings of the 12th Plastic Fuel Gas Pipe Symposium, Boston, USA. 341-342.

DUsclat (1985). Characteristics of a good joint with electrofusion fittings, Proceedings of Plastics Pipes VI, University of York, UK. 31 A 1-8.

M.Fujikake, M.Fukumura and K.Kitao (1997). Analysis of the electrofusion joining process in polyethylene gas piping systems, Computers & Structures, 64, 939-948.

M. F.Kanninen, G.S.Buczala, C.J.Kuhlman, S.T.Green, S.C.Grigory, P.E.O'Donoghue and M. A.McCarthy (1992). A theoretical and experimental evaluation of the long term integrity of an
electrofusion joint, \Proceedings of Plastics Pipes VIII, Koningshof, Netherlands, B2/3.1-10.

G.L.Pitman (1985). Electrofusion welding prediction and computer-aided design of fittings, Proceedings of Plastics Pipes VI, University of York, UK. 29.1-7.

D.Dufour and E. Meister (1989). Polyethylene electrofusion technique: Prediction model of welding quality, \Proc. Int. Gas Resources Conf., Japan, 232-242.

D.Saint-Royre, D.Gueugnaut and D.Reveret (1989). Test methodology for the determination of optimum fusion welding conditions of polyethylene, J. Applied Polymer Science, 38,147-162.

M.Nussbaum, D.Dufour and D.Gueugnaut (1991). Electrofusion of polyethylene: how and why, Proceedings of the 12th Plastic Fuel Gas Pipe Symposium, Boston, USA. 324-330.

T.Nakano, K.Kitao, Y.Yamda, S.Imura and S.Akiyama (1989). Strength evaluation of electrofusion joints in polyethylene gas piping system, Proceedings of the 11th Plastic Fuel Gas Pipe Symposium, 112-126.

A.Nakashiba, H.Nishimura and F.Inoue (1993). Fusion simulation of electrofusion joints for gas distribution, Polym. Eng. Sci., \textbf{33}, 1146-1151.

H.~Nishimura, F.~Inoue and T.~Ishikawa (1992). Fusion simulation of electrofusin joints, Proceedings of the International Gas Resources Conference, Japan. 495-502.

H.~Nishimura, F.~Inoue, A.~Nakashiba and T. Ishikawa (1994). Design of electrofusion joints and evaluation of fusion strength using fusion simulation technology, Polym. Eng. Sci., 34, 1529-1534.

A.S.~Wood, G.F.~Rosala, A.J.~Day, I. Torsun and N.~Dib (1994). Variable grid model for thermoelastic deformation, in Advanced Computational Methods in Heat Transfer III (ed. L.C.~Wrobel, C.A.~Brebbia and A.J.~Nowak), CMP, Southampton, UK. 481-488.

Dey, S.K. and Dey, C. (1983). An explicit predictor-corrector solver with applications to Burgers's equation, in NASA Technical Memo 84402, NASA-Ames Research Centre, Moffett Field, CA.

Osman, H. and Wood, A.S. (2001). Stability of Charlie's method on linear heat conduction equation. Matematik, Jabatan matematik, Fakulti Sains UTM. 1-6.